

1 **Cortico-thalamic tremor circuits and their associations** 2 **with deep brain stimulation effects in essential tremor**

3 **Running Title: Cortico-thalamic circuits and DBS in ET**

4 Shenghong He^{1,2,*}, Timothy O West^{1,2,3}, Fernando R Plazas^{1,2}, Laura Wehmeyer^{1,2,4}, Alek
5 Pogosyan^{1,2}, Alceste Deli^{1,5}, Christoph Wiest^{1,2}, Damian M Herz^{1,2,6}, Thomas Simpson^{1,2},
6 Pablo Andrade⁴, Fahd Baig⁵, Michael G Hart⁵, Francesca Morgante⁵, James J. FitzGerald^{2,7},
7 Michael T Barbe⁴, Veerle Visser-Vandewalle⁴, Alexander L Green^{2,7}, Erlick A Pereira⁵,
8 Hayriye Cagnan^{1,2,3,#}, Huiling Tan^{1,2,#}

9 1 Medical Research Council Brain Network Dynamics Unit, University of Oxford, Oxford, UK

10 2 Nuffield Department of Clinical Neurosciences, University of Oxford, Oxford, UK

11 3 Department of Bioengineering, Imperial College London, London, UK

12 4 Department of Stereotactic and Functional Neurosurgery, University Hospital Cologne, and Faculty
13 of Medicine, University of Cologne, Cologne, Germany

14 5 Neurosciences and Cell Biology Institute, Neuromodulation and Motor Control section, St.
15 George's, University of London, London, UK

16 6 Section of Movement Disorders and Neurostimulation, Department of Neurology, Focus Program
17 Translational Neuroscience (FTN), University Medical Center of the Johannes Gutenberg-University
18 Mainz, Mainz, Germany

19 7 Nuffield Department of Surgical Sciences, University of Oxford, Oxford, UK

20 *For correspondence: Shenghong He, Nuffield Department of Clinical Neurosciences, University of
21 Oxford, 6th Floor West Wing JR Hospital, OX3 9DU (shenghong.he@ndcn.ox.ac.uk)

22 # H.C. and H.T. contributed equally to this study as joint senior authors.

23

24

25

26

27

28

29

30

NOTE: This preprint reports new research that has not been certified by peer review and should not be used to guide clinical practice.

31 **Abstract**

32 Essential tremor (ET) is one of the most common movement disorders in adults. Deep brain
33 stimulation (DBS) of the ventralis intermediate nucleus (VIM) of the thalamus and/or the
34 posterior subthalamic area (PSA) has been shown to provide significant tremor suppression in
35 patients with ET, but with significant inter-patient variability and habituation to the stimulation.
36 Several non-invasive neuromodulation techniques targeting other parts of the central nervous
37 system, including cerebellar, motor cortex, or peripheral nerves, have also been developed for
38 treating ET, but the clinical outcomes remain inconsistent. Existing studies suggest that
39 pathology in ET may emerge from multiple cortical and subcortical areas, but its exact
40 mechanisms remain unclear. By simultaneously capturing neural activities from motor cortices
41 and thalami, and hand tremor signals recorded via accelerometers in fifteen human subjects
42 who have undergone lead implantations for DBS, we systematically characterized the efferent
43 and afferent cortico-thalamic tremor networks. Through the comparisons of these network
44 characteristics and tremor amplitude between DBS OFF and ON conditions, we further
45 investigated the associations between different tremor network characteristics and the
46 magnitude of DBS effect. Our findings implicate the thalamus, specifically the contralateral
47 hemisphere, as the primary generator of tremor in ET, with a significant contribution of the
48 ipsilateral hemisphere as well. Although there is no direct correlation between the cortico-
49 tremor connectivity and tremor power or reduced tremor by DBS, the strength of connectivity
50 from the motor cortex to the thalamus and vice versa at tremor frequency predicts baseline
51 tremor power and effect of DBS. Interestingly, there is no correlation between these two
52 connectivity pathways themselves, suggesting that, independent of the subcortical pathway, the
53 motor cortex appears to play a relatively distinct role, possibly mediated through an
54 afferent/feedback loop in the propagation of tremor. DBS has a greater clinical effect in those
55 with stronger cortico-thalamo-tremor connectivity involving the contralateral thalamus, which
56 is also associated with bigger and more stable tremor measured with an accelerometer.
57 Interestingly, stronger cross-hemisphere coupling between left and right thalami is associated
58 with more unstable tremor. Together this study provides important insights into a better
59 understanding of the cortico-thalamic tremor generating network and its implication for the
60 development of patient-specific therapeutic approaches for ET.

61

62 **Keywords:** Essential tremor, deep brain stimulation, efferent and afferent, directed
63 connectivity, local field potential

64 Introduction

65 Essential tremor (ET) is one of the most common movement disorders in adults, with an
66 estimated prevalence of 0.5-5%.¹⁻³ Based on a series of cortico-cortical, cortico-muscular, and
67 intermuscular coherence analyses, Raethjen and colleagues proposed that tremor in ET
68 emerges from a number of cortical and subcortical motor centres, with each node acting as a
69 dynamically changing oscillator and temporarily entraining each other.⁴⁻⁶ In line with this
70 theory, various neuromodulation techniques targeting distinct brain regions or other
71 components of the central nervous system have been clinically or experimentally employed to
72 treat ET. In clinical practice, high-frequency continuous deep brain stimulation (DBS)
73 specifically targeting the Ventralis Intermedia Nucleus (VIM) of the thalamus has been
74 widely employed and demonstrated significant efficacy in suppressing tremor in patients with
75 ET. Additionally, alternative targets, such as the posterior subthalamic area (PSA, including
76 zona incerta (ZI)), have also been proposed.⁷⁻¹¹ However, despite these promising clinical
77 outcomes, notable inter-patient variability and habituation to the stimulation have been
78 observed. In the realm of experimental non-invasive neuromodulation, several techniques have
79 been developed for treating ET. This includes transcranial alternating/direct current stimulation
80 (TACS/TDCS) targeting cerebellar¹²⁻¹⁴ or motor cortex¹⁵ , repetitive transcranial magnetic
81 stimulation (rTMS) targeting cerebellar¹⁶⁻¹⁸ or motor cortex¹⁹⁻²⁰ , and electrical stimulation
82 targeting peripheral nerves²¹⁻²² , although the clinical outcomes remain inconsistent. To
83 optimize the efficacy of both invasive and non-invasive neuromodulatory approaches, a more
84 precise understanding of the underlying mechanisms driving tremor in ET is needed. This
85 entails elucidating the intricate interplay of multiple cortical and subcortical brain regions
86 involved in the pathophysiology of ET.⁴⁻⁶ However, most of the existing studies are only based
87 on recordings from a single node in the motor circuit (cortical or subcortical) and lack within-
88 subject pre- and post-intervention comparisons. Thus, the characteristics of cortical- and
89 subcortico-tremor networks as well as how they change with intervention targeting the relevant
90 nodes are still unclear.

91 In this study, based on the simultaneous recording of cortical EEG, thalamic local field
92 potentials (LFPs), and limb acceleration measurements from patients with ET, we characterized
93 cortico-thalamo-tremor networks through a directed connectivity analysis called generalized
94 Orthogonalized Partial Directed Coherence (gOPDC),²³ and explored the associations between
95 cortico-thalamo-tremor network characteristics and hand tremor characteristics. Furthermore,
96 based on the data recorded during DBS OFF and DBS ON from each individual participant,

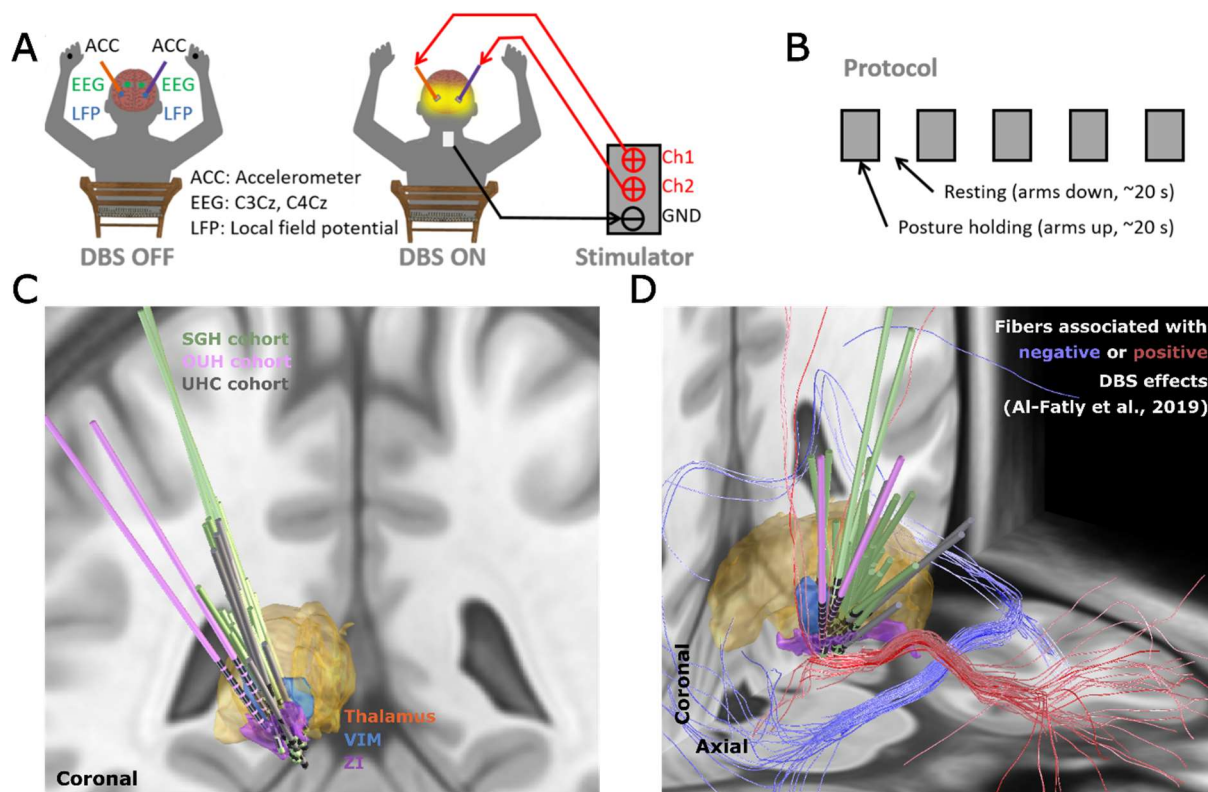
97 we further investigated how the cortico-thalamo-tremor network characteristics predict DBS
98 effect in tremor suppression.

99

100 **Materials and methods**

101 **Human subjects and experimental protocol**

102 Fifteen patients (mean age = 69.1 ± 7.26 years; mean disease duration = 21.1 ± 14.5 years; six
103 females) with ET that underwent DBS surgery (30 DBS leads) participated in this study (P1-
104 P7 and P12 were published previously).²⁴ All participants underwent bilateral implantations of
105 DBS electrodes targeting the VIM thalamus and/or PSA/ZI area. The experimental protocol
106 involved a posture holding task performed while sitting comfortably in a chair, with both arms
107 raised up to the height of shoulders (**Fig. 1A**). The task was performed in blocks in both DBS
108 OFF and ON conditions, with each block lasted about 20 s. There was a resting period when
109 both arms were put down between two posture holding blocks (**Fig. 1B**). In average, the posture
110 holding task was performed for 195.92 ± 11.54 s (mean \pm SEM) and 196.67 ± 14.76 s in DBS
111 OFF and ON conditions, respectively. The study was approved by the local ethics committees
112 and all participants provided their informed written consent according to the Declaration of
113 Helsinki. Clinical details of all participants are summarised in **Table I**.



114

115 **Figure 1. Experimental protocol. (A)** Schematic of the posture holding task performed when the DBS
 116 is switched OFF (left) and ON (right). **(B)** Timeline for the experimental protocol which consists of 10
 117 posture holding blocks (~20 s per block) when both arms are raised up, and 10 resting blocks when both
 118 arms are put down. **(C)-(D)** 3D reconstruction in coronal (C) and coronal-axial (D) views of all analyzed
 119 DBS leads localized in standard Montreal Neurological Institute (MNI)-152_2009b space using Lead-
 120 DBS.²⁵⁻²⁶ Electrodes in the left hemisphere were mirrored to the right hemisphere. UHC = University
 121 Hospital Cologne; OUH = Oxford University Hospital; SGH = St George’s Hospital; VIM = ventral
 122 intermediate thalamus; ZI = zona incerta.

123

124 **Table 1 Clinical details of all recorded participants**

P	G	Age (yr)	DD (yr)	DBS lead	L/R Amp (mA)	Centre	DBS Targeting	Diagnose	Predominant symptom(s) before surgery
1 ^o	F	76-80	21	Abb	1.1/NA	SGH	VIM-PSA	ET	Tremor, gait ataxia, tremor worse on right, upper limb and voice tremor
2 ^o	M	61-65	20	Abb	NA/3	SGH	VIM-PSA	ET	Tremor, dystonia, upper limb tremor and head tremor
3	M	71-75	18	Abb	2.5/2.0	SGH	VIM-PSA	ET	Tremor, upper limb, lower limb and head tremor
4	M	66-70	8	Abb	1.8/1.8	SGH	VIM-PSA	ET	Tremor, upper limb, with right worse than left, lower limb tremor
5	F	61-65	45	Abb	2/2	SGH	VIM-PSA	ET	Tremor, upper limb tremor left worse than right, voice tremor
6	M	66-70	5	Abb	3/3	SGH	VIM-PSA	ET	Tremor, upper limb left worse than right
7	M	66-70	47	Abb	1.5/1.5	SGH	VIM-PSA	ET	Tremor, upper limb right worse than left, head tremor
8 ^o	M	76-80	50	Abb	2.0/2.0	SGH	VIM-PSA	ET	Upper limb action tremor Left > right
9 ^o	F	76-80	14	Abb	2.0/2.0	SGH	VIM-PSA	ET	Upper and lower limb tremor (right > left)
10	F	76-80	20	Bos ¹	2.0/1.5	SGH	VIM-PSA	ET	Upper limbs tremor (right > left)
11	M	71-75	15	Abb	1.0/1.0	SGH	VIM-PSA	ET	Upper limbs tremor (right > left)
12	F	61-65	UN	Bos ²	1.1/1.5	OUH	VIM	ET	Tremor, upper limb, worse intention tremor on left
13 ^o	F	56-60	15	Med	1.5/1.5	UHC	VIM	ET	Tremor in both hands (L>R)
14 ^o	M	51-55	8	Bos ³	NA/2.0	UHC	VIM	ET	Tremor left hand
15	M	71-75	10	Med	3.5/1.2	UHC	VIM	ET	Tremor in both hands (R>L), head tremor
Mean /		66-70	21.1 /		1.85 /	/	/	/	/
SD /		/	14.5 /		0.56 /	/	/	/	/

125

126 P = patient; G = gender; M = male; F = female; yr = year; DD = disease duration; DBS = Deep brain stimulation;
127 Abb = Abbott infinity 1.5mm spaced directional leads (1-4), Abbott; Bos¹ = Boston Cartesia™ HX leads with 3-
128 3-3-3-1-1-1-1 configuration, Boston Scientific; Bos² = Boston linear 8 contact leads (1-8), Boston Scientific; Med
129 = Medtronic SenSight™ directional leads; Bos³ = Boston Vercise™ directional lead with 1-3-3-1 configuration,
130 Boston Scientific; L = left; R = right; Amp = amplitude; NA: Not applicable; SGH = St George’s Hospital; OUH
131 = Oxford University Hospital; UHC = University Hospital Cologne; VIM = ventral intermediate thalamus;
132 PSA = Posterior subthalamic area; ET = essential tremor; SD = standard deviation; * Only unilateral DBS
133 were applied; ^o Tremor from only one hand was recorded; Patient 1 had gait ataxia which is sometimes seen in
134 advanced ET. Patient 2 had an overlap between ET and dystonic tremor.

135

136 **Stimulation**

137 Stimulation was applied bilaterally (except for P1, P2, and P14 who received unilateral
138 stimulation contralateral to the tremor dominant hand) using a highly configurable custom-
139 built neurostimulator or a CE marked stimulator (Inomed, Germany, or Bionics, Australia). In
140 this study, monopolar stimulation was delivered with a fixed stimulation frequency of 130 Hz,
141 a pulse width of 60 μ s, and an interphase gap of 20 μ s. These parameters are illustrated in
142 **Supplementary Figure 1**. Here, the interphase gap is the time between the anodic and cathodic
143 phases used in biphasic stimulation, previously shown to increase stimulation efficiency and
144 reduce battery consumption.²⁷⁻³⁰ The stimulation reference was connected to an electrode patch
145 attached to the back of the participant (**Fig. 1A**). These stimulation parameters and
146 configurations were selected based on previous literature.^{24,31-33} The stimulation contact was
147 selected as following: 1) contact levels targeting VIM-PSA area based on imaging data and/or
148 feedback from neurosurgeon after operation were initially considered. 2) Among them, a
149 contact searching procedure was applied to select the final stimulation contact for each
150 hemisphere. Specifically, we delivered continuous DBS initially at 0.5 mA, then progressively
151 increased the amplitude in 0.5 mA increments, until clinical benefit was seen without side
152 effects such as paraesthesia, or until 3.5 mA was reached as the maximum amplitude. In
153 average, the amplitude used in this study was 1.89 ± 0.12 mA (mean \pm SEM). Details of the
154 stimulation configuration for each participant are summarised in **Table I**.

155

156 **Data recording**

157 Recordings from fifteen participants were conducted 1 to 5 days after the electrode
158 implantation, when the DBS leads were temporarily externalized. While performing the posture
159 holding task illustrated in **Fig. 1**, bilateral LFPs, EEGs covering “Cz”, “C3”, “C4”, “CPz”,

160 “CP3”, and “CP4” according to the standard 10–20 system, and limb accelerations acquired
161 using tri-axial accelerometers taped to the back of both hands were simultaneously recorded
162 using a Porti (TMS International) amplifier at a sampling rate of 2048 Hz (for P1-P7, and P12),
163 or a Saga amplifier (TMS International) at a sampling rate of 4096 Hz (for P8-P11, and P13-
164 P15). When a Porti amplifier was used, the segmented contacts were first constructed in ring
165 mode, then LFPs from two adjacent levels or two levels neighbouring the stimulation contact
166 were recorded in the differential bipolar mode, to avoid saturation during stimulation. While
167 LFPs from each individual contact were recorded in monopolar mode when a Saga amplifier
168 was used, as it has a much higher tolerance of DC offset that may induce saturation during
169 stimulation. Due to lack of tremor on the other hand after DBS surgery, limb accelerations were
170 recorded only from one hand for six (P1-P2, P8-P9, and P13-P14) out of the 15 participants
171 (**Table 1**), resulting in 24 tremulous upper limbs.

172

173 **Data analysis**

174 *Pre-processing*

175 For the LFPs recorded in monopolar mode, bipolar signals were achieved offline by
176 differentiating the recordings from two adjacent contacts or two contacts neighbouring the
177 stimulation contact. In the cases with directional leads, only the contact pairs facing the same
178 direction were considered. For the recorded EEGs, bipolar signals were constructed offline by
179 differentiating between “C3” and “Cz” (i.e., “C3Cz”), or “C4” and “Cz” (i.e., “C4Cz”). The
180 bipolar LFPs and EEGs as well as the recorded acceleration measurements were band-pass
181 filtered at 1–95 Hz and then band-stop filtered at 48-52 Hz using two 4th order zero-phase
182 Butterworth IIR digital filters in MATLAB (R2023-b, MathWorks). After filtering, a principal
183 component analysis (PCA) was applied on the tri-axial acceleration measurements, and the first
184 component was selected as the measurement of tremor on a given hand. PCA components
185 reflect a linear combination of the three (orthogonal) axes, with the first component reflecting
186 the orientation that captures the maximum variance in the data. This technique has precedence
187 in previous studies.^{13,34} To consider the natural intra-individual tremor variability during
188 posture holding (**Fig. 2A**), we split the data into non-overlapping 2 s segments and considered
189 each segment as a trial. This procedure resulted in 98.0 ± 5.8 (mean \pm SEM) and 98.3 ± 7.4
190 trials per subject in DBS OFF and DBS ON conditions, respectively.

191

192 *Spectral analysis*

193 After pre-processing, power spectral density (PSD) was estimated using Welch's overlapped
194 segment averaging estimator for each individual LFPs, EEGs, and acceleration measurements
195 in each trial,³⁵ in a frequency range of 1 to 95 Hz with a 0.5 Hz resolution. To select the tremor
196 frequency for each hand in each trial, we first normalized the PSD of the acceleration
197 measurement against the sum of the power between 1 and 25 Hz, then the frequency between
198 3 and 10 Hz that has the maximum power was selected as the tremor frequency. To select one
199 bipolar LFP for each hemisphere, we averaged the normalized PSD across trials for each
200 bipolar LFP channel, and selected the one with maximum power at the averaged tremor
201 frequency of both tremor hands. Furthermore, for each trial (i.e., 2-s segment), the normalized
202 PSD and power (raw and normalized) at the tremor frequency were calculated for EEGs
203 (“C3Cz” and “C4Cz”), acceleration measurements (left and right hand), and the selected
204 bipolar LFPs for further analysis.

205

206 *Tremor instability analysis*

207 After pre-processing, tremor amplitude and frequency instability in each trial were quantified
208 for each hand. Specifically, the acceleration measurements were high- and low-pass filtered at
209 3 and 10 Hz using two sixth order zero-phase Butterworth IIR digital filters, and z-score
210 normalized. Then, zero-crossing points from negative to positive were used to identify
211 individual tremor cycle within each trial. For each tremor cycle, the instantaneous tremor
212 amplitude was quantified as the distance between the peak and trough, while instantaneous
213 tremor frequency was defined as the reciprocal of the duration of the tremor cycle, as shown in
214 **Fig. 2B**. Finally, tremor amplitude and frequency instability were quantified as the standard
215 deviation of the instantaneous tremor amplitude and frequency across cycles. Please note that
216 with z-score normalization, these represent how stable the tremor is in terms of amplitude and
217 frequency within the 2-s segment, as demonstrated in Supplementary Fig. 2. Tremor stability
218 index^{13,34} and multiscale entropy (MSE)³⁶ have previously been proposed to distinguish ET
219 and parkinsonian tremor. Thus these measurements were also computed for comparison.

220

221 *Connectivity analysis*

222 Based on the simultaneously recorded cortical, subcortical, and tremor signals, we investigated
223 the cortico-thalamo-tremor network characteristics through a directional connectivity analysis
224 using a method called generalized orthogonalized partial directed coherence (gOPDC)

225 developed by Omidvarnia et al.^{23,37} In this method, signal power was first orthogonalized
226 before quantifying coherence, to mitigate the effect of volume conduction.³⁸ Briefly, a
227 coefficient of a multivariate autoregressive (MVAR) model was converted to the spectral
228 domain using the Fourier transform, and then used to calculate the power spectral density
229 matrix. Prior to frequency domain conversation, the MVAR coefficients were
230 orthogonalized.³⁷ This effectively minimizes shared variance between the autoregressive
231 components of the signals, such that correlations arise from off-diagonal terms (i.e.,
232 connectivity). Further details can be found in Omidvarnia et al.^{23,37} Only the imaginary part of
233 the orthogonalized partial directed coherence (OPDC) was considered to reduce spurious
234 correlations introduced by factors such as movement/tremor artefact. In addition, the scale
235 invariant version of the classical PDC (i.e., gOPDC) was used to handle numerical problems
236 associated with different variance of signal amplitudes in LFPs, EEGs, and acceleration
237 measurements (known as time-series scaling).³⁹⁻⁴⁰ This method has been shown to reliably
238 detect event-related directional information flow at ~10 Hz based on non-overlapping 1-s
239 segments of neonatal EEGs.²³ In the current study, we are mainly interested in the tremor
240 frequency band at 3-8 Hz thus the data was truncated into 2-s non-overlapping segments. Based
241 on gOPDC, the mean efferent (from cortices/thalamus to tremor) and afferent (from tremor
242 back to cortices/thalamus) connectivity in a frequency range covering 2 Hz around the basic
243 tremor frequency as well as 2 Hz around the second harmonic frequency were analysed.
244 Furthermore, direct and indirect causal effects of a certain structure were explored by
245 comparing the unconditioned versus conditioned gOPDC models, i.e., excluding or including
246 the corresponding source.²³ Each gOPDC measurement was compared against its surrogate
247 distribution. To this end, the pre-processed continuous tremor time-series was divided into two
248 segments according to a randomly selected point (with a minimum of 2 s margin on each side)
249 and then swapped back and forth to disrupt the coupling between EEG/LFP and tremor signals.
250 Then, the shuffled data were truncated into non-overlapping 2 s trials. This procedure was
251 repeated until we got 1000 trials of shuffled data. The same gOPDC metrics were derived from
252 the shuffled data, resulting in a surrogate distribution of 1000 values per measurement.⁴¹ This
253 approach ensured that any signatures of connectivity remaining, following disruption of the
254 EEG/LFP and tremor signal pairs, arose from the independent statistics of each signal.

255

256 *Spatial distributions of the connectivity measurements*

257 Lead placements were confirmed by fusion of preoperative MRI and postoperative CT scans,
258 which were further established by reconstructing the electrode trajectories and location of
259 different contacts using the Lead-DBS MATLAB toolbox (version 2.6.0).²⁵ The electrode
260 locations were registered and normalized into the Montreal Neurologic Institute (MNI) 152-
261 2009b space using the Connectomic ET Target Atlas.¹¹ As shown in Fig. 1C and D, most of
262 the tested electrodes targeted the VIM-PSA area, close to the fibers, suggested to provide
263 positive DBS effects in tremor patients.¹¹ To investigate the spatial distributions of the
264 bidirectional gOPDC connectivity (thalamo-cortical and cortico-thalamic) and their
265 associations with different targets for ET, we repeated the connectivity analyses for all
266 available bipolar LFP channels from all patients, and mapped them onto the MNI space based
267 on the coordinates of each contact. In addition, for each hemisphere, the volume of tissue
268 activated (VTA) during stimulation was estimated using a finite element method (FEM),²⁵
269 based on the individual electrode position used for the connectivity calculation and a common
270 stimulation amplitude (i.e., 1 mA). Subsequently, the intersections between the VTA and
271 different subcortical structures (e.g., VIM and ZI) were quantified and used to correlate with
272 different connectivity measurements.

273

274 **Statistical analysis**

275 Statistical analyses were conducted using custom-written scripts in MATLAB R2023-b (The
276 MathWorks Inc, Nantucket, MA).

277

278 To compare the PSD of EEGs, LFPs, and acceleration measurements between DBS OFF and
279 DBS ON conditions, a non-parametric cluster-based permutation procedure (repeated 2000
280 times) was applied, in which multiple comparisons were controlled theoretically.⁴²

281

282 To compare the tremor characteristics (power, amplitude instability, and frequency instability)
283 or gOPDC measurements quantified on a trial-by-trial basis between different conditions (e.g.,
284 DBS OFF versus DBS ON, unconditioned versus conditioned gOPDC models, or real gOPDC
285 versus its null distribution), generalized linear mixed effect (GLME) modelling was used.⁴³⁻⁴⁴
286 We also used GLME to further investigate the associations between gOPDC measurements
287 and tremor characteristics on a trial-by-trial basis. In each GLME model, the slope(s) between
288 the predictor(s) and the dependent variable were set to be fixed across all tremor hands while
289 a random intercept was set to vary by hand. The parameters were estimated based on maximum-

290 likelihood using Laplace approximation, the Akaike information criterion (AIC), estimated
291 value with standard error of the coefficient ($k \pm SE$), multiple comparisons corrected P -value
292 and proportion of variability in the response explained by the fitted model (R^2) were reported.
293 Here multiple comparisons applied to different measurements were corrected using
294 false discovery rate (FDR) approach.⁴⁵⁻⁴⁶

295

296 To explore the correlations between different tremor characteristics or gOPDC measurements
297 and the effect of DBS in tremor suppression, or between different gOPDC measurements,
298 Pearson correlation was applied on a hand-by-hand basis. For each correlation analysis, the
299 pairwise linear correlation coefficient (r), multiple comparisons corrected P -value (based on
300 FDR), and sample size (N) were reported. Here the sample size was equal to the number of
301 tremulous upper limbs ($N=24$), unless outliers were identified according to the Pauta criterion
302 (3σ criterion).

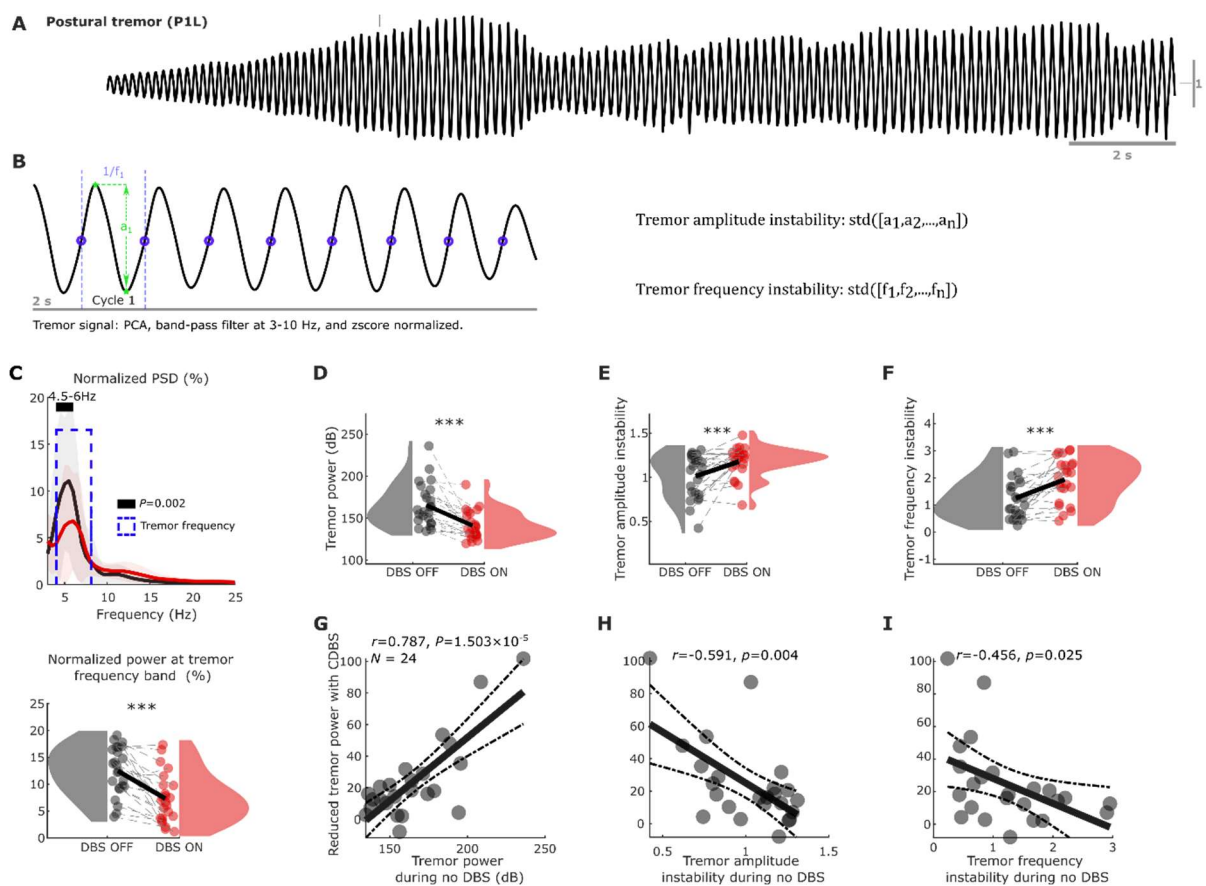
303

304 **Results**

305 **1. Continuous DBS reduces tremor power and stability, and the** 306 **DBS effect correlates with baseline tremor power and instability**

307 The amplitude of postural tremor in ET is unstable over time,⁴⁷⁻⁵⁰ as shown in **Fig. 2A**, which
308 motivated us to quantify tremor characteristics including power at tremor frequencies (peak
309 frequency ± 1 Hz), tremor amplitude instability, and frequency instability in non-overlapping
310 2 s epochs, as shown in **Fig. 2B** (with more details in Methods). As expected, there was a
311 significant reduction in tremor power during DBS ON compared with DBS OFF (**Fig. 2C**, PSD
312 at 4.5-6 Hz: $t = 3.799$, $P = 0.002$; normalized power at individualized tremor frequency band:
313 $k = -5.280 \pm 0.120$, $P < 1 \times 10^{-4}$; **Fig. 2D**, absolute power at individualized tremor frequency
314 band: $k = -26.502 \pm 0.621$, $P < 1 \times 10^{-4}$), although tremor-frequency peaks were identified in
315 both DBS OFF and DBS ON conditions. This was accompanied by a significant power
316 reduction at the tremor frequency band in the VIM thalamic LFPs (**Supplementary Fig. 3A**
317 **and B**) and cortical EEGs (**Supplementary Fig. 3C and D**). In addition, DBS significantly
318 increased the instabilities of tremor amplitude (**Fig. 2E**, $k = 0.173 \pm 0.011$, $P < 1 \times 10^{-4}$) and
319 frequency (**Fig. 2F**, $k = 0.744 \pm 0.029$, $P < 1 \times 10^{-4}$). Here k indicates estimated value with
320 standard error of the coefficient using generalized linear mixed effect (GLME) modelling
321 (Methods). Apart from an expected positive correlation between the level of tremor reduction

322 with DBS and the baseline tremor power during DBS OFF (**Fig. 2G**, $r = 0.787$, $P = 1.50 \times 10^{-5}$), baseline tremor instability was also found to be negatively correlated with the effect of DBS
 323 ⁵), baseline tremor instability was also found to be negatively correlated with the effect of DBS
 324 (**Fig. 2H**, amplitude instability, $r = -0.591$, $P = 0.004$; **Fig. 2I**, frequency instability, $r = -0.456$,
 325 $P = 0.025$). We repeated this analysis using two other tremor instability measurements
 326 including TSI^{13,34} and MSE³⁶. As shown in **Supplementary Fig. 4**, these measurements were
 327 highly correlated with each other and showed similar relationships with respect to the effect of
 328 DBS. Together, these suggested that more severe and stable tremor during DBS OFF was
 329 associated with a larger effect of DBS on tremor reduction.



330

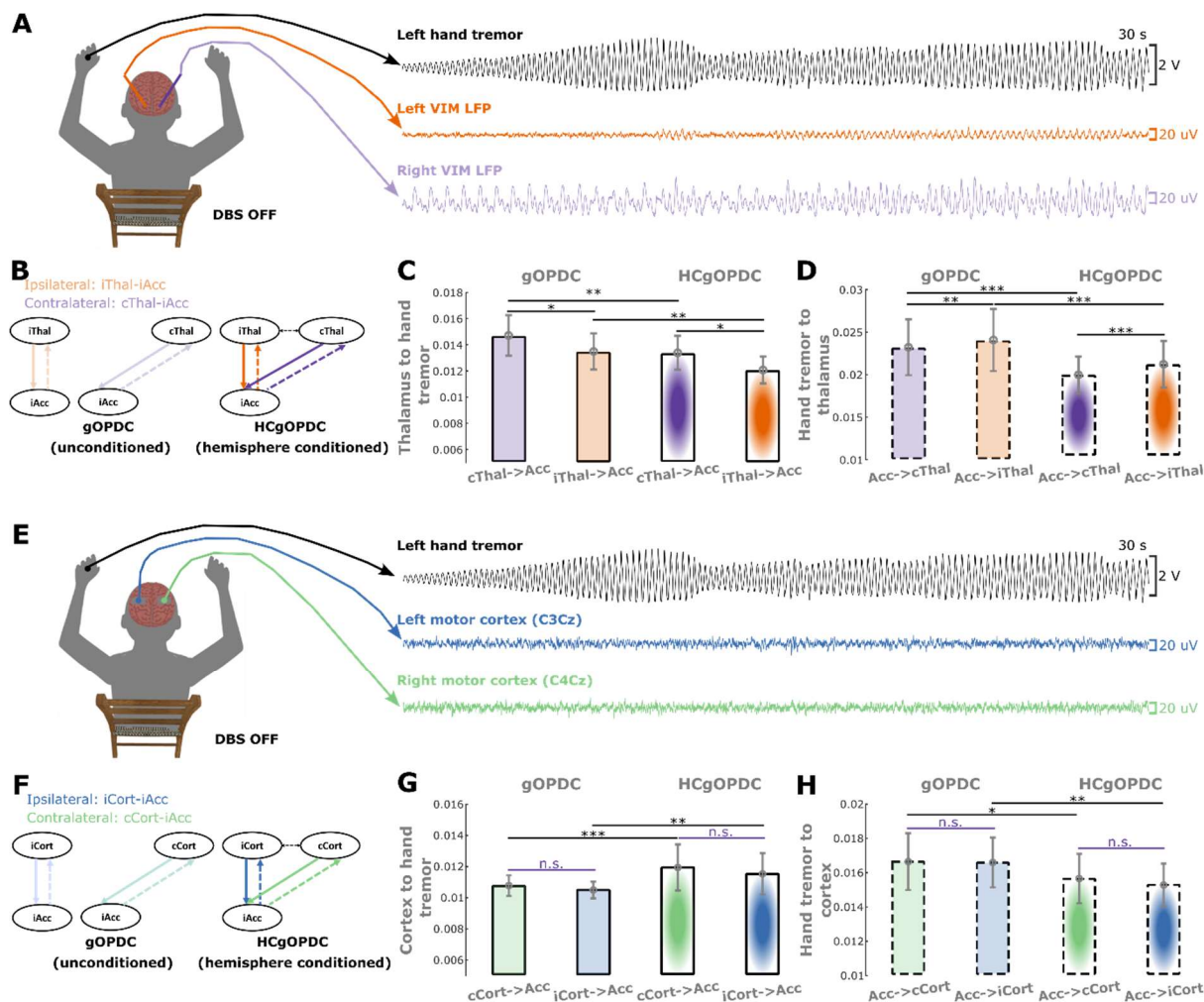
331 **Figure 2. Comparisons of tremor characteristics between DBS OFF and DBS ON conditions. (A)**
 332 **An example of 30-s postural tremor (P1L) showing the instability of tremor in ET. (B)** Demonstration
 333 of the quantifications of tremor amplitude and frequency instability from a segment of 2 s measurement
 334 from an accelerometer. **(C)** Normalized power spectral density (PSD) of accelerometer measurements
 335 showed peaks at tremor frequency band in both DBS OFF (black) and DBS ON (red) conditions (upper
 336 panel), with a significant reduction of the normalized power (in percentage) in the individualized tremor
 337 frequency band during DBS ON (lower panel). **(D)-(F)** Comparisons of tremor power (D), amplitude
 338 instability (E), and frequency instability (F) between DBS OFF (black) and DBS ON (red) conditions
 339 using raincloud plots.⁵¹ Here the shaded areas indicate distributions (probability density) of the data.
 340 **(G)-(I)** Tremor power during DBS OFF (baseline) positively (G) while tremor amplitude (H) and
 341 frequency (I) instability negatively correlated with the reduction in tremor power during DBS (Pearson
 342 correlation). Solid lines in C and bars in C-F indicate mean, while shaded areas in C and error bars in
 343 C-F indicate standard error of the mean (SEM). Statistics were applied between DBS OFF and DBS
 344 ON conditions using a nonparametric cluster-based permutation procedure in C (PSD) on a hand-by-
 345 hand basis, or using generalized linear mixed effect modelling in all bar plots (C-F) on a trial-by-trial

346 basis. Multiple comparisons were corrected by controlling the false discovery rate (FDR). *** $P < 0.001$
347 after FDR correction.
348

349 **2. The efferent and afferent thalamic-tremor networks are both** 350 **lateralized and interact across hemispheres**

351 Based on the simultaneously recorded hand acceleration measurements and bilateral thalamic
352 LFPs during posture holding (**Fig. 3A**), we characterized bidirectional connectivity between
353 VIM thalamus and hand tremor in the tremor frequency band (2 Hz around the peak tremor
354 frequency as well as 2 Hz around the second harmonic frequency) using generalized
355 Orthogonalized Partial Directed Coherence (gOPDC, with details in Methods). As shown in
356 **Supplementary Table 1**, we first tested the main effects of laterality (contralateral versus
357 ipsilateral), cross-hemisphere coupling (conditioned versus unconditioned), and directionality
358 (efferent versus afferent), as well as the interaction effects between them. This analysis
359 revealed significant main effects for all these conditions and significant interaction effects
360 between laterality and directionality, as well as between cross-hemisphere coupling and
361 directionality. We then conducted pairwise comparisons and the results revealed that without
362 DBS, the efferent connectivity from the contralateral thalamus to hand tremor was significantly
363 stronger than that from the ipsilateral thalamus (**Fig. 3C**, unconditioned model, $k = -0.001 \pm$
364 0.001 , $P = 0.029$; hemisphere conditioned model, $k = -0.001 \pm 0.001$, $P = 0.011$), as expected.
365 However, the afferent network showed an opposite pattern, with a significantly stronger input
366 from hand tremor to the ipsilateral thalamus than that to the contralateral thalamus (**Fig. 3D**,
367 unconditioned model, $k = 0.002 \pm 0.001$, $P = 0.001$; hemisphere conditioned model, $k = 0.003$
368 ± 0.001 , $P = 4.73 \times 10^{-5}$). Overall, the strength of the afferent network was stronger than the
369 efferent network. This thalamic-tremor network laterality disappeared during DBS
370 (**Supplementary Fig. 5**). Compared with the model only involving unilateral (either
371 contralateral or ipsilateral) thalamus and hand tremor (**Fig. 3B left**, unconditioned model),
372 conditioning the impact from the other thalamus (hemisphere conditioned model, **Fig. 3B right**)
373 significantly reduced the efferent connectivity from both the contralateral (**Fig. 3C**, $k = -0.002$
374 ± 0.001 , $P = 0.004$) and ipsilateral (**Fig. 3C**, $k = -0.002 \pm 0.001$, $P = 0.002$) thalami to hand
375 tremor. Similarly, the afferent connectivity from hand tremor to both the contralateral (**Fig. 3D**,
376 $k = -0.004 \pm 0.001$, $P = 7.88 \times 10^{-11}$) and ipsilateral (**Fig. 3D**, $k = -0.004 \pm 0.001$, $P = 2.91 \times$
377 10^{-8}) thalami were also significantly reduced in the hemisphere conditioned model compared
378 with unconditioned model. This suggests that there was cross-hemisphere coupling between
379 the two thalami in the thalamic-tremor network. During DBS, the hemisphere conditioned

380 model also significantly reduced the efferent connectivity from both thalami to hand tremor,
 381 but not the afferent connectivity from hand tremor to both thalami (**Supplementary Fig. 5**).
 382 The details of the GLME models used for these tests were summarized in **Supplementary**
 383 **Table 1**.



384
 385 **Figure 3. Characteristics of thalamic-tremor and cortico-tremor networks when DBS was**
 386 **switched off. (A)** A demonstration of left-hand postural tremor and thalamic LFP recordings from
 387 participant 1, left hand (P1L) during DBS OFF condition. **(B)** Directed connectivity between VIM
 388 thalamus and hand tremor quantified using generalized Orthogonalized Patial Directed Coherence
 389 (gOPDC). Solid lines indicate efferent connectivity from thalamus to hand tremor, while dashed lines
 390 indicate afferent connectivity from hand tremor to thalamus. Orange and purple represent the
 391 connectivity with ipsilateral and contralateral VIM thalami, respectively. The upper and lower panels
 392 indicate gOPDC involving only one thalamus (unconditioned) and both thalami (hemisphere
 393 conditioned: HCgOPDC), respectively. **(C)** Efferent connectivity from the contralateral thalamus was
 394 significantly stronger than that from the ipsilateral hemisphere in both unconditioned (left) and
 395 hemisphere conditioned (right) models. When conditioning the impact from the other hemisphere, the
 396 efferent connectivity from the contralateral (purple) and ipsilateral (orange) thalami to hand tremor were
 397 both significantly reduced. **(D)** Afferent connectivity from hand tremor to the contralateral thalamus
 398 was significantly weaker than that to the ipsilateral hemisphere in both unconditioned (left) and
 399 hemisphere conditioned (right) models. When conditioning the impact from the other hemisphere, the
 400 afferent connectivity from hand tremor to the contralateral (purple) and ipsilateral (orange) thalami were
 401 both significantly reduced. **(E)-(H)** The same as (A)-(D) but for cortico-tremor network. Bars and error
 402 bars indicate mean and standard error of the mean (SEM), respectively. Statistics were applied on each

403 comparison using generalized linear mixed effect modelling on a trial-by-trial basis. Multiple
404 comparisons were corrected by controlling the false discovery rate (FDR). * $P < 0.05$; ** $P < 0.01$; ***
405 $P < 0.001$; after FDR correction.
406

407 **3. The efferent and afferent cortico-tremor networks are non-** 408 **lateralized but interact across hemispheres**

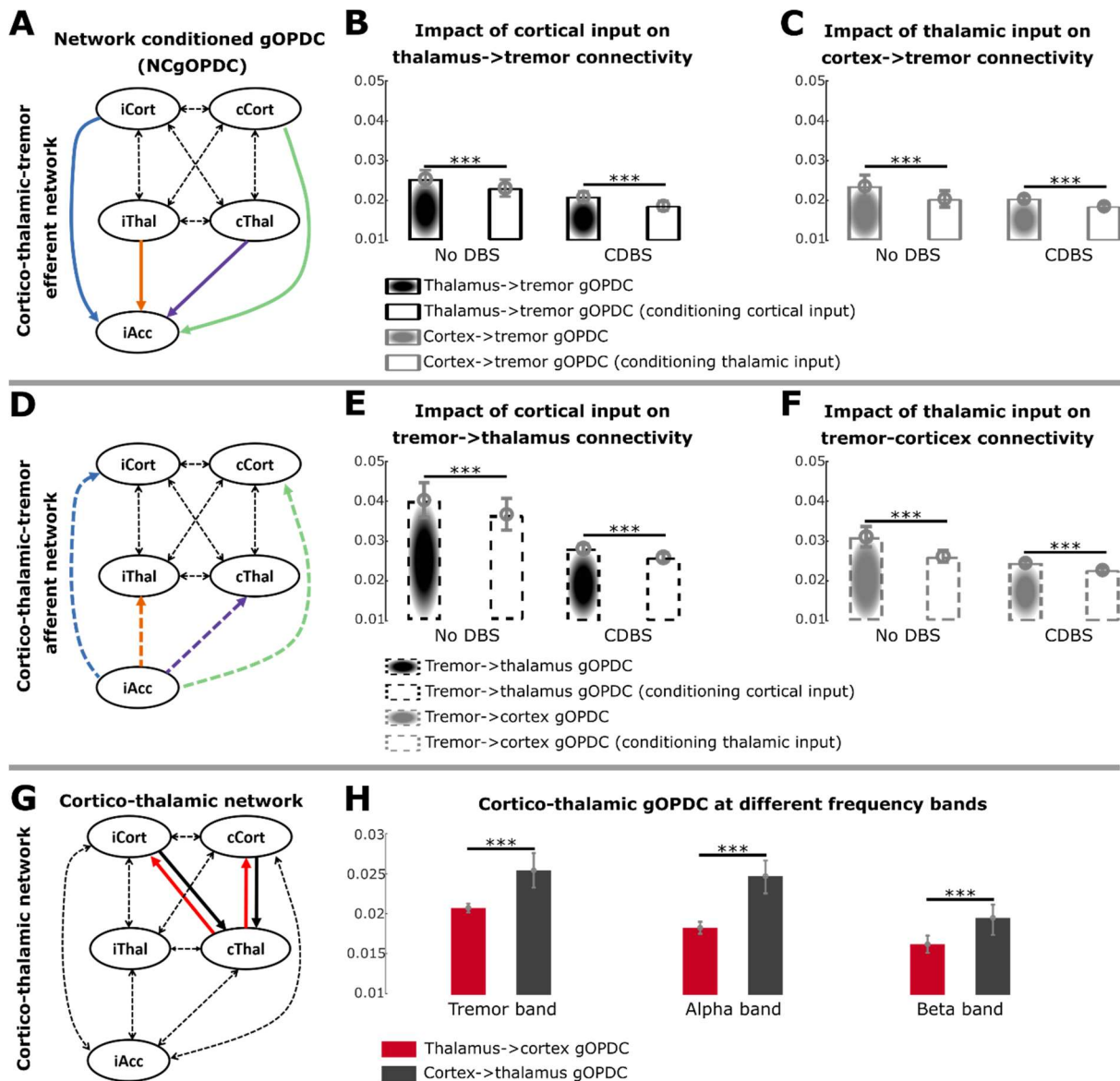
409 Based on the simultaneously recorded hand acceleration measurements and EEGs from
410 bilateral sensorimotor cortices during posture holding (**Fig. 3E**), we characterized bidirectional
411 (efferent and afferent) connectivity between cortical activities and hand tremor in the tremor
412 frequency band using gOPDC. Similarly, we first identified significant main effects on cross-
413 hemisphere coupling and directionality, but not on laterality. The interaction between cross-
414 hemisphere coupling and directionality was also significant (Supplementary Table 2). We then
415 conducted pairwise comparisons and the results. We then conducted pairwise comparisons and
416 the results revealed that without DBS, there was no significant difference between the efferent
417 connectivity from the contralateral and ipsilateral motor cortices to hand tremor in either the
418 unconditioned (**Fig. 3G**) or hemisphere-conditioned model. Similar results were observed in
419 the afferent tremor to cortical connectivity (**Fig. 3H**). Compared with the model only involving
420 unilateral sensorimotor cortex and hand tremor (**Fig. 3F left**, unconditioned model),
421 conditioning the impact from the other cortex (conditioned model, **Fig. 3F right**) significantly
422 increased the efferent connectivity from both the contralateral (**Fig. 3G**, $k = 0.001 \pm 4 \times 10^{-4}$,
423 $P = 9.0 \times 10^{-4}$) and ipsilateral (**Fig. 3G**, $k = 0.001 \pm 4 \times 10^{-4}$, $P = 0.003$) sensorimotor cortices
424 to hand tremor. However, the afferent connectivity from hand tremor to both the contralateral
425 (**Fig. 3H**, $k = -0.001 \pm 0.001$, $P = 0.030$) and ipsilateral (**Fig. 3H**, $k = -0.001 \pm 4 \times 10^{-4}$, $P =$
426 0.007) cortices reduced significantly in the conditioned model compared with unconditioned
427 model. During DBS, none of these comparisons were significant (**Supplementary Fig. 6**).
428 These results suggest that the cortico-tremor network is not lateralized but interacts across
429 hemispheres, in other words, there is coupling between the ipsilateral and contralateral cortices,
430 and both of them contribute to hand tremor equally. The details of the GLME models used for
431 these tests were summarized in **Supplementary Table 2**.

432

433 **4. Interaction between the thalamic-tremor and cortico-tremor** 434 **networks**

435 To investigate the potential relationship between the thalamic-tremor and cortico-tremor
436 networks, we included the simultaneously recorded hand tremor, bilateral thalamic LFPs, and

437 cortical EEGs in a single gOPDC model (network conditioned gOPDC: NCgOPDC). By
438 comparing the efferent connectivity strength achieved from this network conditioned model
439 (**Fig. 4A**) against those achieved from the gOPDC model only involving thalamic (**Fig. 3B**) or
440 cortical (**Fig. 3E**) sources, we found that when conditioning the cortical inputs, the efferent
441 connectivity from thalamus to hand tremor was significantly reduced (**Fig. 4B**, DBS OFF, $k =$
442 -0.002 ± 0.001 , $P = 8.75 \times 10^{-4}$; DBS ON, $k = -0.002 \pm 0.001$, $P = 9.25 \times 10^{-6}$). Vice versa,
443 conditioning thalamic inputs significantly reduced the efferent connectivity from cortex to hand
444 tremor (**Fig. 4C**, DBS OFF, $k = -0.003 \pm 0.001$, $P = 3.57 \times 10^{-7}$; DBS ON, $k = -0.002 \pm 0.001$,
445 $P = 2.35 \times 10^{-6}$). Similarly, the afferent connectivity from hand tremor to thalamus (**Fig. 4E**,
446 DBS OFF, $k = -0.004 \pm 0.001$, $P = 5.60 \times 10^{-6}$; DBS ON, $k = -0.002 \pm 0.001$, $P = 5.05 \times 10^{-5}$)
447 or cortex (**Fig. 4F**, DBS OFF, $k = -0.006 \pm 0.001$, $P < 1 \times 10^{-4}$; DBS ON, $k = -0.002 \pm 0.001$,
448 $P = 2.67 \times 10^{-4}$) in the network conditioned model (**Fig. 4D**) was also significantly reduced
449 compared with the gOPDC model only involving thalamic (**Fig. 3B**) or cortical (**Fig. 3E**)
450 sources. These results suggest that the thalamic-tremor and cortico-tremor networks interact
451 with each other, in line with the theory proposed by Raethjen et al.⁴⁻⁶ When directly comparing
452 the connectivity from thalamus to cortex versus the connectivity from cortex to thalamus (**Fig.**
453 **4G**), we found that the connectivity from cortex to thalamus was significantly stronger than
454 the connectivity in the other direction (from thalamus to cortex, **Fig. 4H**). The results were
455 similar for either tremor ($k = 0.005 \pm 0.001$, $P = 3.60 \times 10^{-17}$), alpha ($k = 0.007 \pm 0.001$, $P =$
456 9.89×10^{-29}), or beta ($k = 0.004 \pm 4 \times 10^{-4}$, $P = 9.59 \times 10^{-23}$) frequency bands.



457

458 **Figure 4. Characteristics of cortico-thalamo-tremor network.** (A) Directed efferent connectivity
 459 from sensorimotor cortex and VIM thalamus to hand tremor quantified using generalized
 460 Orthogonalized Patial Directed Coherence (gOPDC). (B) Comparing with the model only involving
 461 bilateral thalami in Fig. 3, conditioning cortical input significantly reduced the efferent connectivity
 462 from thalamus to hand tremor in both DBS OFF and DBS ON conditions. (C) Comparing with the
 463 model only involving bilateral sensorimotor cortices in Fig. 3, conditioning thalamic input significantly
 464 reduced the efferent connectivity from cortex to hand tremor in both DBS OFF and DBS ON conditions.
 465 (D) Directed afferent connectivity from hand tremor to sensorimotor cortex and VIM thalamus
 466 quantified using gOPDC. (E) Comparing with the model only involving bilateral thalami in Fig. 3,
 467 conditioning cortical input significantly reduced the afferent connectivity from hand tremor to thalamus
 468 in both DBS OFF and DBS ON conditions. (F) Comparing with the model only involving bilateral
 469 sensorimotor cortices in Fig. 3, conditioning thalamic input significantly reduced the afferent
 470 connectivity from hand tremor to cortex in both DBS OFF and DBS ON conditions. Here the
 471 connectivity in (A)-(F) was quantified in tremor frequency band. (G) Directed connectivity between
 472 sensorimotor cortices and the contralateral VIM thalamus relative to the focused hand tremor quantified
 473 using gOPDC. (H) The directed top-down connectivity from cortex to thalamus (black) was
 474 significantly and consistently stronger than bottom-up connectivity from thalamus to cortex (red) in
 475 tremor (left), alpha (middle), and beta (right) frequency bands. Bars and error bars indicate mean and
 476 standard error of the mean (SEM), respectively. Statistics were applied on each comparison using

477 generalized linear mixed effect modelling on a trial-by-trial basis. Multiple comparisons were corrected
478 by controlling the false discovery rate (FDR). *** $P < 0.001$ after FDR correction.

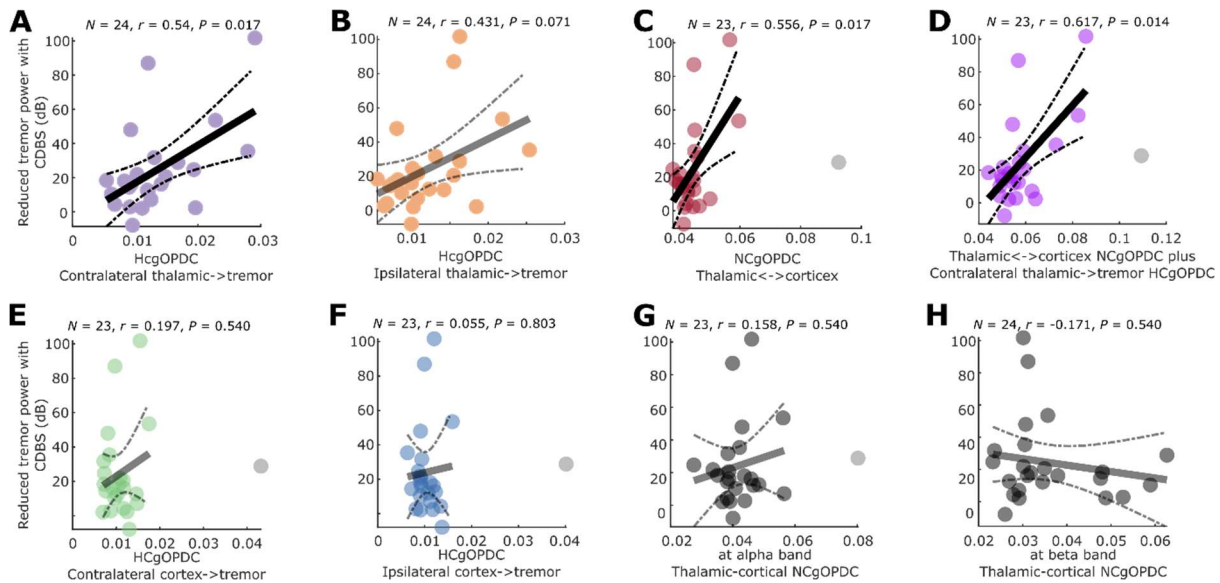
479
480

481 **5. Connectivity involving contralateral thalamus positively**

482 **correlates with DBS effect**

483 To further investigate whether the cortico-thalamo-tremor network characteristics could be
484 used to predict the effect on tremor suppression with VIM DBS, we performed Pearson's
485 correlation analysis between different connectivity measurements and the DBS effect in
486 reducing tremor. This analysis revealed that the efferent connectivity from the contralateral
487 thalamus to hand tremor (**Fig. 5A**, $r = 0.54$, $P = 0.017$) and the overall connectivity strength
488 between thalamus and cortex at tremor frequency (thalamus to cortex plus cortex to thalamus,
489 **Fig. 5C**, $r = 0.556$, $P = 0.017$) positively correlated with the level of tremor power reduction
490 during DBS ON. There was a trend of positive correlation between the efferent connectivity
491 from the ipsilateral thalamus and hand tremor, which however did not survive multiple
492 comparison correction (**Fig. 5B**, $r = 0.431$, $P = 0.071$). Combining all connectivity involving
493 the contralateral thalamus increased the effect size of the positive correlation (**Fig. 5D**, $r =$
494 0.617 , $P = 0.014$). In addition, there was no correlation between the reduced tremor power and
495 the efferent connectivity from either the contralateral (**Fig. 5E**) or ipsilateral (**Fig. 5F**)
496 sensorimotor cortex, or the overall connectivity strength between thalamus and cortex in other
497 frequency bands as control (**Fig. 5G**, alpha band; **Fig. 5H**, beta band). When using generalized
498 linear mixed effect modelling (GLME) to predict tremor power using various connectivity
499 measurements (**Supplementary Table 3** Model 1), only the connectivity involving thalamus
500 including efferent connectivity from contralateral ($k = 94.488 \pm 21.8$, $P = 4.571 \times 10^{-5}$) and
501 ipsilateral ($k = 116.54 \pm 24.651$, $P = 1.44 \times 10^{-5}$) thalami to hand tremor, connectivity from
502 thalamus to cortex ($k = 88.322 \pm 22.94$, $P = 2 \times 10^{-4}$), and connectivity from cortex to thalamus
503 ($k = 41.844 \pm 16.178$, $P = 0.015$) in tremor frequency band showed significant prediction effects,
504 but not the efferent connectivity from sensorimotor cortex to hand tremor. To test if the
505 connectivity measurements are simply representations of electrode locations. We quantified
506 the distances between the selected contacts and a sweetspot in VIM for tremor suppression
507 with DBS suggested in a previous study,¹¹ and correlated them with connectivity measurements
508 and DBS effects. The results showed that the connectivity measurements in **Fig. 5A-D** did not
509 correlate with the distances between contacts and the tremor sweetspot (**Supplementary Fig.**

510 **7A-D)**, but provided better prediction of DBS effects than the distances (**Supplementary Fig.**
 511 **7E).**



512

513 **Figure 5. Correlations between cortico-thalamo-tremor network characteristics and the reduced**
 514 **tremor power with DBS. (A)-(B)** Correlations between the efferent connectivity from the contralateral
 515 (A) or ipsilateral (B) thalami to hand tremor and the reduced tremor power with DBS. (C) Correlation
 516 between the sum of thalamus to cortex and cortex to thalamus connectivity at tremor frequency band
 517 and the reduced tremor power with DBS. (D) Correlation between the sum of all connectivity at tremor
 518 frequency involving the contralateral thalamus and the reduced tremor power with DBS. (E)-(F) There
 519 was no correlation between the efferent connectivity from the contralateral (E) or ipsilateral (F)
 520 sensorimotor cortices to hand tremor and the reduced tremor power with DBS. (G)-(H) There was no
 521 correlation between the sum of thalamus to cortex and cortex to thalamus connectivity at alpha (G) or
 522 beta (H) frequency band and the reduced tremor power with DBS. P-values were corrected for multiple
 523 comparisons by controlling false discovery rate (FDR).
 524
 525

526 **6. Thalamic-tremor connectivity is predicted by tremor** 527 **characteristics**

528 We then used GLME to test if the thalamic-tremor connectivity strength can be predicted by
 529 tremor characteristics (power and instability). This analysis revealed that stronger tremor
 530 power (**Supplementary Table 3 Model 2**, $k = 0.0002 \pm 3.88 \times 10^{-5}$, $P = 9.12 \times 10^{-8}$) and
 531 smaller tremor amplitude instability (indicating more stable tremor, **Supplementary Table 3**
 532 **Model 2**, $k = -0.007 \pm 0.002$, $P = 0.001$) together predicted greater connectivity involving
 533 contralateral thalamus. On the other hand, stronger tremor power (**Supplementary Table 3**
 534 **Model 3**, $k = -0.001 \pm 4 \times 10^{-4}$, $P < 1 \times 10^{-4}$) and greater connectivity involving the contralateral
 535 thalamus (**Supplementary Table 3 Model 3**, $k = -0.685 \pm 0.236$, $P = 0.004$) together predicted
 536 smaller tremor amplitude instability, i.e., more stable hand tremor. These results confirmed that

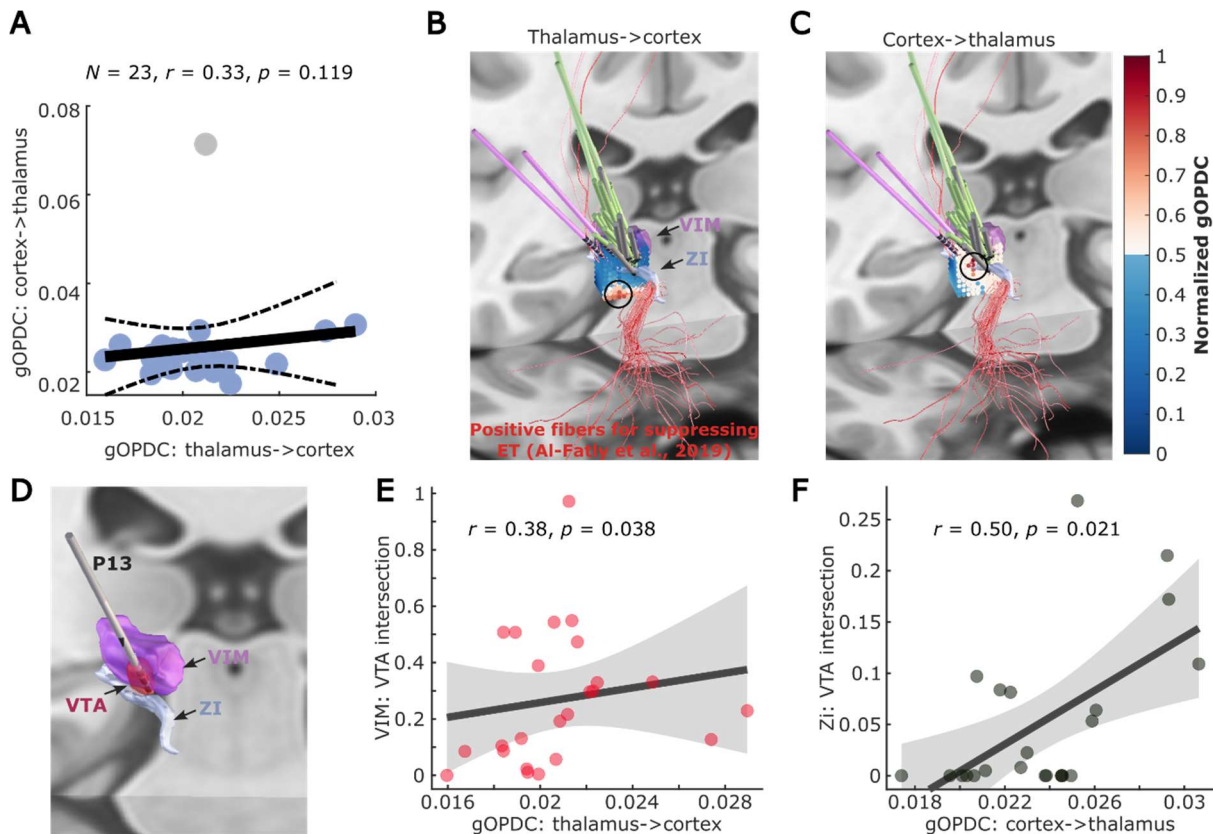
537 there is a clear association between the strength of the functional connectivity involving the
538 contralateral thalamus and tremor characteristics.

539

540 **7. Motor cortex and thalamus have separate pathways in tremor** 541 **propagation**

542 Although the thalamo-cortical and cortico-thalamic connectivity at tremor frequency predicted
543 the DBS effects (**Fig. 5C and D**), there was no correlation between them (**Fig. 6A**). In addition,
544 the strongest thalamo-cortical connectivity and cortico-thalamic connectivity clustered at
545 different areas in the MNI space (**Fig. 6B and C**). These results suggested that the thalamo-
546 cortical and cortico-thalamic connectivity at tremor frequency band may have different spatial
547 sources. Using Lead-DBS, we quantified the VTA during stimulation at 1 mA for each
548 hemisphere, as shown in **Fig. 6D**. Correlation analysis revealed that the intersection between
549 VTA and VIM thalamus positively correlated with the thalamo-cortical connectivity (**Fig. 6E**,
550 $r = 0.38$, $P = 0.038$), but not the cortico-thalamic connectivity ($r = 0.03$, $P = 0.452$) measured
551 from the same contacts. In contrast, the intersection between VTA and ZI positively correlated
552 with the cortico-thalamic connectivity (**Fig. 6F**, $r = 0.50$, $P = 0.021$), but not the thalamo-
553 cortical connectivity ($r = 0.12$, $P = 0.274$). The results were consistent when using 2 mA
554 amplitude for simulation in Lead-DBS. Together, these results suggest that tremor propagation
555 from thalamus to motor cortex mainly involves VIM, while propagation from the motor cortex
556 back to thalamus mainly involves ZI/PSA.

557



558

559 **Figure 6. Comparisons between thalamo-cortical and cortico-thalamic connectivity.** (A) Directed
 560 connectivity at tremor frequency band (gOPDC) from thalamus to cortex (x-axis) did not correlate with
 561 that from cortex to thalamus (y-axis). (B)-(C) The strongest thalamo-cortical (B) and cortico-thalamic
 562 (C) gOPDC clustered at different areas in the standard MNI-152 2009b space. (D) A demonstration of
 563 the volume of tissue activated (VTA) with DBS at 1 mA applied to the selected bipolar LFP channels
 564 (P13). (E) Results from Spearman rank correlation between the intersection of the VTA in VIM
 565 thalamus and directed connectivity from thalamus to cortex. (F) Results from Spearman rank correlation
 566 between the intersection of the VTA in Zi and directed connectivity from cortex to thalamus.

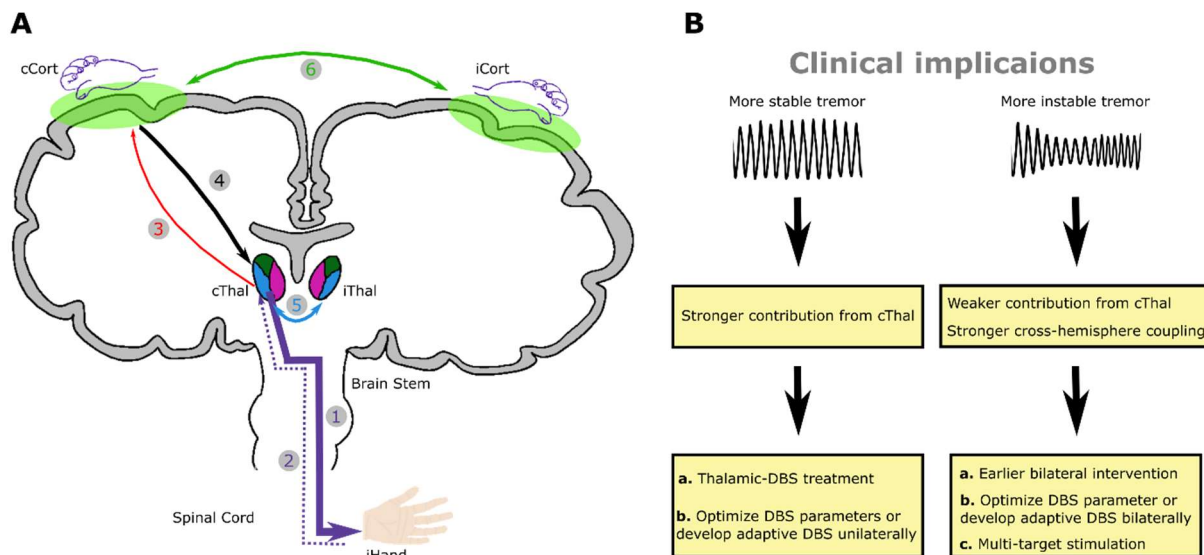
567

568 Discussion

569 In this study, we characterized the cortico-thalamo-tremor network based on hand acceleration
 570 measurements, thalamic LFPs, and cortical EEGs recorded simultaneously from people with
 571 ET during posture holding in both ON and OFF DBS conditions (Fig. 7). Specifically, we have
 572 shown that apart from with a stronger lateralized efferent connectivity from the contralateral
 573 thalamus to hand tremor (as expected), there is also contribution from the ipsilateral thalamus,
 574 as evidenced by significant changes observed in connectivity measurements between thalamus
 575 and hand tremor (efferent and afferent) when partializing out (conditioning) the contribution
 576 made by the ipsilateral thalamus. The lateral asymmetry was not observed in the cortico-tremor
 577 network. Furthermore, although the thalamic-tremor and cortico-tremor networks have
 578 different network characteristics and correlated differently with tremor, they interact with each
 579 other, with significant changes observed in the connectivity when partializing out (conditioning)

580 the contribution made by the other network. Secondly, we have shown that both the tremor
581 power during DBS OFF and the effect of VIM/PSA DBS were only predicted by the
582 connectivity involving the thalamus but not by the cortico-tremor connectivity. In addition, the
583 connectivity involving the contralateral thalamus, which showed the best correlation with the
584 DBS effect, was independently predicted by tremor power and amplitude instability,
585 suggesting both tremor power and tremor instability represent some level of underlying cortico-
586 thalamo-tremor network characteristics. Lastly, although both thalamo-cortical and cortico-
587 thalamic connectivity at tremor frequency band contributed to predicting DBS effect on tremor
588 suppression, there was no correlation between them, suggesting motor cortex and thalamus
589 may have separate pathways in tremor propagation. These results together shed light on the
590 tremor network in ET.

591



592

593 **Figure 7. A summary of the current study. (A)** Our study suggests that tremor in ET originates from
594 the contralateral thalamus (path 1). The motor cortex is involved through an indirect pathway, likely
595 via a feedback loop, by receiving afferent input from the tremulous hand through ascending pathways
596 (paths 2 and 3) and sending it back to the thalamus (path 4). There is also significant cross hemisphere-
597 coupling at both subcortical (path 5) and cortical (path 6) levels. **(B)** Potential clinical implications of
598 this study. cCort=contralateral motor cortex; iCort=ipsilateral motor cortex; cThal=contralateral
599 thalamus; iThal=ipsilateral thalamus.

600

601 Verification of the gOPDC connectivity measurements

602 In this study, the tremor information flow was assessed using partial directed coherence,
603 quantified using a method called gOPDC, which has been suggested to be able to remove
604 common components akin to volume conduction effects. This method addresses the numerical
605 problem associated with different variance of signal amplitudes (here accelerometer
606 measurement, LFP, and EEG), and can detect directed information flow within a subsecond

607 time scale in nonstationary multichannel signals.²³ A variant algorithm of this method (without
608 orthogonalization) has also been used to characterize the cerebello-cortical network between
609 essential, Parkinsonian, and mimicked tremor.⁵² Results of a few tests provide evidence that
610 the quantified gOPDC measurements are physiologically meaningful: 1) along with the
611 reduction of tremor power during DBS, gOPDC measurements were significantly reduced with
612 DBS compared with during DBS OFF (**Supplementary Table 4**), and the laterality of the
613 thalamic-tremor network also disappeared (**Supplementary Fig. 5**); 2) We applied gOPDC to
614 surrogate data by shuffling the tremor measurements relative to LFPs and EEGs. Statistical
615 analysis showed that gOPDC measurements based on real data were all significantly bigger
616 than those derived from surrogate data (**Supplementary Fig. 8** and Method); 3) The presented
617 results were still valid when using the variant algorithm without orthogonalization (i.e., gPDC),
618 which resulted in significantly larger connectivity values but has weaker effect sizes in the
619 thalamic laterality and correlation analysis (**Supplementary Fig. 9**). Please note that the
620 presented thalamic-tremor network laterality phenomenon was not captured by another non-
621 directional connectivity measurement, i.e., imaginary coherence, in which the directionality
622 (i.e., afferent and efferent) and causality are not considered (**Supplementary Fig. 10**).

623

624 **The contralateral thalamus as a main generator of tremor in ET**

625 Existing studies showed that the tremor in ET remains constant when the resonant frequency
626 of the oscillating limb is changed by added inertia.⁵³⁻⁵⁴ Compared with Parkinsonian tremor,
627 tremor in ET has a much narrower frequency tolerance (a measure that characterizes the
628 temporal evolution of tremor by quantifying the range of frequencies over which the tremor
629 may be considered stable), suggesting it has a more finely tuned central drive.^{13,55-56} Thalamic
630 neuronal activity correlated with ET.⁵⁷ Our results showed that only the thalamus-involved
631 connectivity significantly correlated with both the tremor power during DBS OFF and the
632 reduced tremor power during DBS ON, but not the cortico-tremor connectivity strength. Within
633 the central thalamic-tremor network, the efferent connectivity from the contralateral thalamus
634 to hand tremor was significantly stronger than that from the ipsilateral thalamus. This laterality
635 was not due to the selection of analysed bipolar LFP channels, as it persisted when averaging
636 across all bipolar LFP channels within each hemisphere (**Supplementary Fig. 11**). These
637 results are consistent with existing literature showing strong coherence between thalamic LFP
638 and contralateral muscular EMG in ET,⁵⁷ and clinical evidence demonstrating substantial
639 tremor suppression in the contralateral hand following unilateral thalamic DBS.⁵⁸⁻⁵⁹ This

640 evidence suggests that the tremor might originally be generated from the contralateral thalamus.
641 Whaley et al. reported that from a clinical series of 487 consecutive individuals diagnosed with
642 ET, only about half (52%) of the sample reported bilateral initial tremor onset, but eventually
643 about 90% of the individuals presented bilateral tremor.⁶⁰ Here we also found that there was a
644 significant bidirectional cross hemisphere coupling within the thalamic-tremor network,
645 highlighted by the significant changes in the efferent and afferent information flow between
646 the contralateral/ipsilateral thalamus and accelerometer when partializing out the contributions
647 from bilateral information flow (**Fig. 3C and D**). To further investigate if this is physiologically
648 meaningful, we repeated the GLME modelling (Supplementary Table 3) by adding the gOPDC
649 measurements between hemispheres in the models. The results showed that stronger cross-
650 hemisphere communication predicted larger (e.g., power) but more unstable tremor (e.g., larger
651 amplitude and frequency instability) (**Supplementary Table 5**). In addition, the afferent
652 connectivity from hand tremor back to the ipsilateral thalamus was significantly stronger than
653 that to the contralateral thalamus. However, this was only true for the selected bipolar LFP
654 channels but not when averaging across all bipolar channels within each hemisphere
655 (**Supplementary Fig. 11**). Together these results suggest that the ipsilateral thalamus still plays
656 an important role in the development of tremor. Please note that effects of laterality, cross-
657 hemisphere coupling, and correlations between thalamic-tremor connectivity and DBS effects
658 were not driven by the fact that most of the patients included in this study presented bilateral
659 dysfunction: our key results were not impacted when partializing out (conditioning) the
660 contribution made by the other tremulous hand (Supplementary Fig. 12).

661

662 **Cortical involvement in ET**

663 Conflicting results have been reported on the existence of tremor-related cortical activity in
664 ET.⁶¹⁻⁶² Raethjen et al. reported an intermittent loss of corticomuscular coherence at tremor
665 frequency despite strong peripheral tremor constantly present.⁶ Roy et al. showed that
666 providing high visual feedback worsened tremor compared with low feedback.⁶³ Here we found
667 the strength of the bidirectional cortico-thalamic connectivity predicted baseline tremor power
668 during DBS OFF (Supplementary **Table 3**, Model 1) as well as the effect of DBS (**Fig. 5C**).
669 Conditioning either the cortical or thalamic inputs significantly reduced the thalamic-tremor or
670 cortico-tremor connectivity. These results support the presence of cortical involvement in
671 tremor propagation in ET. In addition, we found that the afferent connectivity from hand tremor
672 back to cortex negatively correlated with that to thalamus (Supplementary **Table 3**, Model 4),

673 and the connectivity from cortex to thalamus was significantly stronger than the connectivity
674 from thalamus to cortex, with no clear correlation between them (Supplementary **Table 3**,
675 Model 5; **Fig. 6A**). Furthermore, we quantified cortico-thalamic and thalamo-cortical gOPDC
676 at the tremor frequency band for each individual bipolar LFP channel for all recorded
677 hemispheres, and mapped the values into standard MNI space using the Lead-DBS toolbox.
678 This revealed the strongest cortico-thalamic and thalamo-cortical gOPDC clustered at
679 relatively different areas relative to VIM thalamus, with both close to the fibers suggested to
680 be associated with positive DBS effect in ET (**Fig. 6B-C**).¹¹ Furthermore, simulation analysis
681 revealed that the intersection between the VTA and VIM thalamus correlated with thalamo-
682 cortical gOPDC, but not cortico-thalamic gOPDC. In comparison, the intersection between the
683 VTA and ZI correlated with cortico-thalamic gOPDC, but not thalamo-cortical gOPDC (**Fig.**
684 **6D-F**). There was, however, no correlation between the efferent cortico-tremor connectivity
685 and tremor power or reduced tremor by DBS. Based on these results, we speculate that the
686 cortical involvement in tremor propagation may primarily reflect sensory inputs from the
687 muscles, relayed via ascending tracts like the dorsal column–medial lemniscus (DCML)
688 pathway, incorporating the spinal cord and sensory thalamic areas. This process appears
689 relatively independent from the cerebellar outflow pathways, involving the VIM-PSA region,
690 which is likely more directly involved in tremor generation and is also a common target for
691 DBS in the treatment of ET.^{52,64-65} Further exploration on this would require new data and is
692 outside the scope of this work.

693

694 **Clinical implications**

695 Our results showed that thalamic-tremor connectivity correlated with the DBS effect on tremor
696 suppression (**Fig. 5**). Linear mixed effect modelling revealed that both tremor power and tremor
697 amplitude instability had independent contributions when predicting the directed connectivity
698 involving the contralateral thalamus: more stable tremors associated with greater connectivity
699 involving the thalamus, which predicted a greater DBS effect. This is consistent with previous
700 studies showing that those with more stable tremors benefited more from tremor phase-specific
701 DBS targeting the thalamus,⁶⁶⁻⁶⁷ or phase-specific transcranial electrical stimulation targeting
702 the cerebellum.¹⁴ Our results also highlighted that more unstable tremor was associated with
703 stronger cross-hemisphere coupling. The outcome of DBS in people with ET is heterogeneous
704 with some patients not benefitting from the intervention or developing habituation over time.
705 Lead placement may account for some of this heterogeneity in clinical outcomes. However

706 another important factor to consider is that the clinical syndrome of ET might be underlined by
707 different network characteristics. Indeed, these potential variations in the disease network may
708 necessitate the use of alternative targeting and stimulation modalities. The following clinical
709 implications arise from our study (**Fig. 7**). 1) *Where to stimulate?* Thalamic DBS may be more
710 effective for individuals with larger, more stable tremors since tremors with these
711 characteristics are potentially driven by a more prominent tremor-generating source in the
712 contralateral thalamus. On the other hand, our results suggest that unstable tremor arises from
713 a less focal source and is more likely to involve multiple generators including those in the
714 cortex. This may suggest that more unstable tremors may benefit from alternative surgical
715 targets, such as the PSA or stimulation of multiple regions across the cerebello-thalamo-cortical
716 pathway,^{11,68-69} similar to the strategy that is currently being investigated in chronic pain,
717 involving implantation of electrodes encompassing multiple targets to disrupt the pain-network
718 rather than perturbing a single node.⁷⁰⁻⁷¹ 2) *How to stimulate?* Our results show that patients
719 with unstable tremors exhibit stronger cross-hemisphere coupling. This suggests that
720 implanting DBS bilaterally may be more beneficial in these patients, even in the case that
721 tremor may only initially present in one hand. Moreover, when assessing the effects of DBS
722 on a tremulous hand, optimizing stimulation parameters on both sides may be more beneficial
723 than focusing solely on the contralateral side. 3) *When to stimulate?* Taking into account the
724 variations in the disease network may also be beneficial for the development of a fully
725 embedded closed-loop stimulation system. For instance, for those with more stable tremors, it
726 might be more practical to implement closed-loop stimulation based on the thalamic LFPs.²⁴
727 While for those with more unstable tremors, additional sites might be needed for closed-loop
728 stimulation.⁷²

729

730 **Limitations**

731 There are several limitations in the current study. First, all recordings were conducted 1-6 days
732 after the first surgery of DBS electrode implantations, thus some participants might still
733 experience an appreciable postoperative stun effect, which however is more likely to overall
734 reduce rather than increase the effect size of the reported results. Second, although the
735 associations between tremor and tremor network characteristics were explored on a trial-by-
736 trial basis, the correlations between these characteristics and the effect of DBS were only
737 investigated on a hemisphere basis, due to the lack of data to effectively quantify the reduced

738 tremor in a trial-by-trial basis. Third, although we somehow characterized both thalamic-tremor
739 and cortico-tremor networks, only a thalamus-targeted intervention was applied in this study,
740 thus it is still unclear whether the cortico-tremor network characteristics could be used to
741 predict the effect of cortex-targeted brain stimulation. Furthermore, although tests against
742 surrogate distributions and comparisons between DBS OFF and ON conditions suggest that the
743 cortico-tremor connectivity, quantified based on scalp EEG, is physiologically meaningful, it
744 should be interpreted carefully and the use of intracranial cortical recordings such as
745 electrocorticography (ECoG) should be preferred wherever possible to improve anatomical
746 precision. Finally, we show that the thalamic-tremor network presented both laterality and
747 cross-hemisphere dependency characteristics, but we cannot further investigate the potential of
748 using these characteristics to predict the effect of unilateral DBS, as bilateral stimulation was
749 applied for most of the patients in this study.

750

751 **Data availability**

752 The data and codes will be shared on the data sharing platform of the MRC Brain Network
753 Dynamics Unit: <https://data.mrc.ox.ac.uk/mrcbndu/data-sets/search>.

754

755 **Acknowledgement**

756 This work was supported by the Medical Research Council (MC_UU_00003/2) and the
757 Guarantors of Brain. S.H. was also supported by Royal Society Sino-British Fellowship Trust
758 (IES\R3\213123). We thank all participants for making this study possible, thank Dr Bassam
759 Al-Fatly and Dr Amir Omidvarnia for providing useful discussions on data analysis.

760

761 **References**

762

- 763 1. Brin MF, Koller W. Epidemiology and genetics of essential tremor. *Movement Disorders*.
764 1998;13(S3):55-63. DOI: 10.1002/mds.870131310
- 765 2. Louis ED, Ferreira JJ. How common is the most common adult movement disorder? Update on
766 the worldwide prevalence of essential tremor. *Movement Disorders*. 2010 Apr 15;25(5):534-
767 41. DOI: 10.1002/mds.22838
- 768 3. Dallapiazza RF, Lee DJ, De Vloo P, Fomenko A, Hamani C, Hodaie M, Kalia SK, Fasano A,
769 Lozano AM. Outcomes from stereotactic surgery for essential tremor. *Journal of Neurology*,

- 770 *Neurosurgery & Psychiatry*. 2019 Apr 1;90(4):474-82. doi.org/10.1136/jnnp-2018-318240
- 771 4. Raethjen J, Lindemann M, Schmaljohann H, Wenzelburger R, Pfister G, Deuschl G. Multiple
772 oscillators are causing parkinsonian and essential tremor. *Movement disorders*. 2000
773 Jan;15(1):84-94. DOI: 10.1002/1531-8257(200001)15:1<84::AID-MDS1014>3.0.CO;2-K
- 774 5. Raethjen J, Lindemann M, Morsnowski A, Dümpelmann M, Wenzelburger R, Stolze H, Fietzek
775 U, Pfister G, Elger CE, Timmer J, Deuschl G. Is the rhythm of physiological tremor involved
776 in cortico-cortical interactions?. *Movement Disorders*. 2004 Apr;19(4):458-65. DOI:
777 10.1002/mds.10686
- 778 6. Raethjen J, Govindan RB, Kopper F, Muthuraman M, Deuschl G. Cortical involvement in the
779 generation of essential tremor. *Journal of neurophysiology*. 2007 May;97(5):3219-28.
780 DOI: 10.1152/jn.00477.2006
- 781 7. Lyons KE, Pahwa R, Busenbark KL, Tröster AI, Wilkinson S, Koller WC. Improvements in
782 daily functioning after deep brain stimulation of the thalamus for intractable tremor. *Movement*
783 *disorders*. 1998 Jul;13(4):690-2. DOI: 10.1002/mds.870130414
- 784 8. Obwegeser AA, Uitti RJ, Turk MF, Strongosky AJ, Wharen RE. Thalamic stimulation for the
785 treatment of midline tremors in essential tremor patients. *Neurology*. 2000 Jun 27;54(12):2342-
786 4. DOI: 10.1212/WNL.54.12.2342
- 787 9. Baizabal-Carvallo JF, Kagnoff MN, Jimenez-Shahed J, Fekete R, Jankovic J. The safety and
788 efficacy of thalamic deep brain stimulation in essential tremor: 10 years and beyond. *Journal*
789 *of Neurology, Neurosurgery & Psychiatry*. 2014 May 1;85(5):567-72. DOI: 10.1136/jnnp-
790 2013-304943
- 791 10. Cury RG, Fraix V, Castrioto A, Pérez Fernández MA, Krack P, Chabardes S, Seigneuret E,
792 Alho EJ, Benabid AL, Moro E. Thalamic deep brain stimulation for tremor in Parkinson disease,
793 essential tremor, and dystonia. *Neurology*. 2017 Sep 26;89(13):1416-23.
794 DOI: 10.1212/WNL.0000000000004295
- 795 11. Al-Fatly B, Ewert S, Kübler D, Kroneberg D, Horn A, Kühn AA. Connectivity profile of
796 thalamic deep brain stimulation to effectively treat essential tremor. *Brain*. 2019 Oct
797 1;142(10):3086-98. DOI: 10.1093/brain/awz236
- 798 12. Gironell A, Martínez-Horta S, Aguilar S, Torres V, Pagonabarraga J, Pascual-Sedano B,
799 Ribosa-Nogué R. Transcranial direct current stimulation of the cerebellum in essential tremor:
800 a controlled study. *Brain Stimulation*. 2014 May 1;7(3):491-2. DOI: 10.1016/j.brs.2014.02.001
- 801 13. Brittain JS, Cagnan H, Mehta AR, Saifee TA, Edwards MJ, Brown P. Distinguishing the central
802 drive to tremor in Parkinson's disease and essential tremor. *Journal of Neuroscience*. 2015 Jan
803 14;35(2):795-806. DOI: 10.1523/JNEUROSCI.3768-14.2015
- 804 14. Schreglmann SR, Wang D, Peach RL, Li J, Zhang X, Latorre A, Rhodes E, Panella E, Cassara
805 AM, Boyden ES, Barahona M. Non-invasive suppression of essential tremor via phase-locked
806 disruption of its temporal coherence. *Nature communications*. 2021 Jan 13;12(1):363. DOI:

- 807 10.1038/s41467-020-20581-7
- 808 15. Brittain JS, Probert-Smith P, Aziz TZ, Brown P. Tremor suppression by rhythmic transcranial
809 current stimulation. *Current Biology*. 2013 Mar 4;23(5):436-40. DOI:
810 10.1016/j.cub.2013.01.068
- 811 16. Gironell A, Kulisevsky J, Lorenzo J, Barbanoj M, Pascual-Sedano B, Otermin P. Transcranial
812 magnetic stimulation of the cerebellum in essential tremor: a controlled study. *Archives of*
813 *neurology*. 2002 Mar 1;59(3):413-7. DOI: 10.1001/archneur.59.3.413
- 814 17. Popa T, Russo M, Vidailhet M, Roze E, Lehericy S, Bonnet C, Apartis E, Legrand AP, Marais
815 L, Meunier S, Gallea C. Cerebellar rTMS stimulation may induce prolonged clinical benefits
816 in essential tremor, and subjacent changes in functional connectivity: an open label trial. *Brain*
817 *stimulation*. 2013 Mar 1;6(2):175-9. DOI: 10.1016/j.brs.2012.04.009
- 818 18. Olfati N, Shoeibi A, Abdollahian E, Ahmadi H, Hoseini A, Akhlaghi S, Vakili V, Foroughipour
819 M, Rezaeitalab F, Farzadfard MT, Layegh P. Cerebellar repetitive transcranial magnetic
820 stimulation (rTMS) for essential tremor: A double-blind, sham-controlled, crossover, add-on
821 clinical trial. *Brain stimulation*. 2020 Jan 1;13(1):190-6. DOI: 10.1016/j.brs.2019.10.003
- 822 19. Hellriegel H, Schulz EM, Siebner HR, Deuschl G, Raethjen JH. Continuous theta-burst
823 stimulation of the primary motor cortex in essential tremor. *Clinical neurophysiology*. 2012
824 May 1;123(5):1010-5. DOI: 10.1016/j.clinph.2011.08.033
- 825 20. Badran BW, Glusman CE, Austelle CW, Jenkins S, DeVries WH, Galbraith V, Thomas T,
826 Adams TG, George MS, Revuelta GJ. A double-blind, sham-controlled pilot trial of pre-
827 supplementary motor area (Pre-SMA) 1 Hz rTMS to treat essential tremor. *Brain Stimulation*.
828 2016 Nov 1;9(6):945-7. DOI: 10.1016/j.brs.2016.08.003
- 829 21. Reis C, Arruda BS, Pogosyan A, Brown P, Cagnan H. Essential tremor amplitude modulation
830 by median nerve stimulation. *Scientific Reports*. 2021 Sep 6;11(1):17720.
- 831 22. Shukla AW. Rationale and evidence for peripheral nerve stimulation for treating essential
832 tremor. *Tremor and other hyperkinetic movements*. 2022;12. DOI: 10.5334/tohm.685
- 833 23. Omidvarnia A, Azemi G, Boashash B, O'Toole JM, Colditz PB, Vanhatalo S. Measuring time-
834 varying information flow in scalp EEG signals: orthogonalized partial directed coherence. *IEEE*
835 *transactions on biomedical engineering*. 2013 Oct 18;61(3):680-93. DOI:
836 10.1109/tbme.2013.2286394
- 837 24. He S, Baig F, Mostofi A, Pogosyan A, Debarros J, Green AL, Aziz TZ, Pereira E, Brown P,
838 Tan H. Closed - loop Deep Brain Stimulation for essential tremor based on thalamic local field
839 potentials. *Movement Disorders*. 2021a Apr;36(4):863-73. DOI: 10.1002/mds.28513
- 840 25. Horn A, Li N, Dembek TA, et al. Lead-DBS v2: towards a comprehensive pipeline for deep
841 brain stimulation imaging. *Neuroimage*. 2019;184:293-316. DOI:
842 10.1016/j.neuroimage.2018.08.068

- 843 26. Avants BB, Epstein CL, Grossman M, Gee JC. Symmetric diffeomorphic image registration
844 with cross-correlation: evaluating automated labeling of elderly and neurodegenerative brain.
845 *Medical image analysis*. 2008 Feb 1;12(1):26-41. DOI: 10.1016/j.media.2007.06.004
- 846 27. Hofmann L, Ebert M, Tass PA, Hauptmann C. Modified pulse shapes for effective neural
847 stimulation. *Frontiers in neuroengineering*. 2011 Sep 28;4:9.
- 848 28. Popovych OV, Lysyansky B, Tass PA. Closed-loop deep brain stimulation by pulsatile delayed
849 feedback with increased gap between pulse phases. *Scientific reports*. 2017 Apr 21;7(1):1033.
- 850 29. Krauss JK, Lipsman N, Aziz T, Boutet A, Brown P, Chang JW, Davidson B, Grill WM, Hariz
851 MI, Horn A, Schulder M, Mammis A, Tass PA, Volkmann J, Lozano AM. Technology of deep
852 brain stimulation: current status and future directions. *Nature Reviews Neurology*. 2021
853 Feb;17(2):75-87.
- 854 30. Gilbert Z, Mason X, Sebastian R, Tang AM, Del Campo-Vera RM, Chen KH, Leonor A, Shao
855 A, Tabarsi E, Chung R, Sundaram S,
856 Kammen A, Cavaleri J, Gogia AS, Heck C, Nune G, Liu CY, Kellis SS, Lee B. A review of
857 neurophysiological effects and efficiency of waveform parameters in deep brain stimulation.
858 *Clinical Neurophysiology*. 2023 Aug 1;152:93-111.
- 859 31. Little S, Pogosyan A, Neal S, et al. Adaptive deep brain stimulation in advanced Parkinson
860 disease. *Ann Neurol* 2013; 74: 449–457. DOI: 10.1002/ana.23951
- 861 32. Debarros J, Gaignon L, He S, Pogosyan A, Benjaber M, Denison T, Brown P, Tan H. Artefact-
862 free recording of local field potentials with simultaneous stimulation for closed-loop deep-brain
863 stimulation. In 2020 42nd Annual International Conference of the IEEE Engineering in
864 Medicine & Biology Society (EMBC) 2020 Jul 20 (pp. 3367-3370). IEEE.
- 865 33. He S, Baig F, Merla A, Torrecillos F, Perera A, Wiest C, Debarros J, Benjaber M, Hart MG,
866 Ricciardi L, Morgante F, Hasegawa H, Samuel M, Edwards M, Denison T, Pogosyan A,
867 Ashkan K, Pereira E, Tan H, Beta-triggered adaptive deep brain stimulation during reaching
868 movement in Parkinson's disease, *Brain*, 2023 Dec; 146(12):5015-30. DOI:
869 10.1093/brain/awad233
- 870 34. Di Biase L, Brittain JS, Shah SA, Pedrosa DJ, Cagnan H, Mathy A, Chen CC, Martín-Rodríguez
871 JF, Mir P, Timmerman L, Schwingenschuh P. Tremor stability index: a new tool for differential
872 diagnosis in tremor syndromes. *Brain*. 2017 Jul 1;140(7):1977-86. DOI: 10.1093/brain/awx104
- 873 35. Welch P. The use of fast Fourier transform for the estimation of power spectra: a method based
874 on time averaging over short, modified periodograms. *IEEE Transactions on audio and*
875 *electroacoustics*. 1967 Jun;15(2):70-3. DOI: 10.1109/TAU.1967.1161901
- 876 36. Su D, Zhang F, Liu Z, Yang S, Wang Y, Ma H, Manor B, Hausdorff JM, Lipsitz LA, Pan H,
877 Feng T, Zhou J. Different effects of essential tremor and Parkinsonian tremor on multiscale
878 dynamics of hand tremor. *Clinical Neurophysiology*. 2021 Sep 1;132(9):2282-9.
- 879 37. Omidvarnia AH, Azemi G, Boashash B, Toole JM, Colditz P, Vanhatalo S. Orthogonalized

- 880 partial directed coherence for functional connectivity analysis of newborn EEG. In *Neural*
881 *Information Processing: 19th International Conference, ICONIP 2012, Doha, Qatar, November*
882 *12-15, 2012, Proceedings, Part II 19 2012 (pp. 683-691). Springer Berlin Heidelberg.*
- 883 38. Hipp JF, Hawellek DJ, Corbetta M, Siegel M, Engel AK. Large-scale cortical correlation
884 structure of spontaneous oscillatory activity. *Nature neuroscience*. 2012 Jun;15(6):884-90. DOI:
885 10.1038/nn.3101
- 886 39. Baccala LA, Sameshima K, Takahashi DY. Generalized partial directed coherence. In *2007*
887 *15th International conference on digital signal processing 2007 Jul 1 (pp. 163-166). Ieee.* DOI:
888 10.1109/ICDSP.2007.4288544
- 889 40. Faes L, Nollo G. Extended causal modeling to assess Partial Directed Coherence in multiple
890 time series with significant instantaneous interactions. *Biological cybernetics*. 2010
891 Nov;103:387-400. DOI: 10.1007/s00422-010-0406-6
- 892 41. He S, Deli A, Fischer P, Wiest C, Huang Y, Martin S, Khawaldeh S, Aziz TZ, Green AL,
893 Brown P, Tan H. Gait-phase modulates alpha and beta oscillations in the pedunculopontine
894 nucleus. *Journal of Neuroscience*. 2021b Oct 6;41(40):8390-402. DOI:
895 10.1523/JNEUROSCI.0770-21.2021
- 896 42. Maris E, Oostenveld R. Nonparametric statistical testing of EEG-and MEG-data. *Journal of*
897 *neuroscience methods*. 2007 Aug 15;164(1):177-90. DOI: 10.1016/j.jneumeth.2007.03.024
- 898 43. Lo S, Andrews S. To transform or not to transform: Using generalized linear mixed models to
899 analyse reaction time data. *Frontiers in psychology*. 2015 Aug 7;6:1171. DOI:
900 10.3389/fpsyg.2015.01171
- 901 44. Yu Z, Guindani M, Grieco SF, Chen L, Holmes TC, Xu X. Beyond t test and ANOVA:
902 applications of mixed-effects models for more rigorous statistical analysis in neuroscience
903 research. *Neuron*. 2022 Jan 5;110(1):21-35. DOI: 10.1016/j.neuron.2021.10.030
- 904 45. Benjamini Y, Hochberg Y. Controlling the false discovery rate: a practical and powerful
905 approach to multiple testing. *Journal of the Royal statistical society: series B (Methodological)*.
906 1995 Jan;57(1):289-300. DOI: 10.1111/j.2517-6161.1995.tb02031.x
- 907 46. Benjamini Y, Yekutieli D. The control of the false discovery rate in multiple testing under
908 dependency. *Annals of statistics*. 2001 Aug 1:1165-88.
- 909 47. Bain PG, Findley LJ, Atchison P, Behari M, Vidailhet M, Gresty M, Rothwell JC, Thompson
910 PD, Marsden CD. Assessing tremor severity. *Journal of Neurology, Neurosurgery &*
911 *Psychiatry*. 1993 Aug 1;56(8):868-73. DOI: 10.1136/jnnp.56.8.868
- 912 48. Britton TC, Thompson PD, Day BL, Rothwell JC, Findley LJ, Marsden CD. Rapid wrist
913 movements in patients with essential tremor: the critical role of the second agonist burst. *Brain*.
914 1994 Feb 1;117(1):39-47. DOI: 10.1093/brain/117.1.39
- 915 49. Brittain JS, Cagnan H, Mehta AR, Saifee TA, Edwards MJ, Brown P. Distinguishing the central
916 drive to tremor in Parkinson's disease and essential tremor. *Journal of Neuroscience*. 2015 Jan

- 917 14;35(2):795-806. DOI: 10.1523/JNEUROSCI.3768-14.2015
- 918 50. Weerasinghe G, Duchet B, Cagnan H, Brown P, Bick C, Bogacz R. Predicting the effects of
919 deep brain stimulation using a reduced coupled oscillator model. *PLoS computational biology*.
920 2019 Aug 8;15(8):e1006575. DOI: 10.1371/journal.pcbi.1006575
- 921 51. Allen M, Poggiali D, Whitaker K, Marshall TR, van Langen J, Kievit RA. Raincloud plots: a
922 multi-platform tool for robust data visualization. *Wellcome open research*. 2019;4.
- 923 52. Muthuraman M, Raethjen J, Koirala N, Anwar AR, Mideksa KG, Elble R, Groppa S, Deuschl
924 G. Cerebello-cortical network fingerprints differ between essential, Parkinson's and mimicked
925 tremors. *Brain*. 2018 Jun 1;141(6):1770-81. DOI: 10.1093/brain/awy098
- 926 53. Elble RJ. Physiologic and essential tremor. *Neurology*. 1986 Feb 1;36(2):225-225. DOI:
927 10.1212/WNL.36.2.22
- 928 54. Deuschl G, Krack P, Lauk M, Timmer J. Clinical neurophysiology of tremor. *Journal of clinical
929 neurophysiology*. 1996 Mar 1;13(2):110-21. DOI: 10.1097/00004691-199603000-00002
- 930 55. Brittain JS, Brown P. The many roads to tremor. *Experimental neurology*. 2013 Dec 1;250:104-
931 7. DOI: 10.1016/j.expneurol.2013.09.012
- 932 56. Hua SE, Lenz FA, Zirh TA, Reich SG, Dougherty PM. Thalamic neuronal activity correlated
933 with essential tremor. *Journal of Neurology, Neurosurgery & Psychiatry*. 1998 Feb
934 1;64(2):273-6. DOI: 10.1136/jnnp.64.2.273
- 935 57. Pedrosa DJ, Quatuor EL, Reck C, Pauls KA, Huber CA, Visser-Vandewalle V, Timmermann
936 L. Thalamomuscular coherence in essential tremor: hen or egg in the emergence of tremor?.
937 *Journal of Neuroscience*. 2014 Oct 22;34(43):14475-83. DOI: 10.1523/JNEUROSCI.0087-
938 14.2014
- 939 58. Ondo W, Jankovic J, Schwartz K, Almaguer M, Simpson RK. Unilateral thalamic deep brain
940 stimulation for refractory essential tremor and Parkinson's disease tremor. *Neurology*. 1998 Oct
941 1;51(4):1063-9. DOI: 10.1212/wnl.51.4.1063
- 942 59. Huss DS, Dallapiazza RF, Shah BB, Harrison MB, Diamond J, Elias WJ. Functional assessment
943 and quality of life in essential tremor with bilateral or unilateral DBS and focused ultrasound
944 thalamotomy. *Movement Disorders*. 2015 Dec;30(14):1937-43. DOI: 10.1002/mds.26455
- 945 60. Whaley NR, Putzke JD, Baba Y, Wszolek ZK, Uitti RJ. Essential tremor: phenotypic
946 expression in a clinical cohort. *Parkinsonism & related disorders*. 2007 Aug 1;13(6):333-9.
947 DOI: 10.1016/j.parkreldis.2006.12.004
- 948 61. Halliday DM, Conway BA, Farmer SF, Shahani U, Russell AJ, Rosenberg JR. Coherence
949 between low-frequency activation of the motor cortex and tremor in patients with essential
950 tremor. *The Lancet*. 2000 Apr 1;355(9210):1149-53. DOI: 10.1016/s0140-6736(00)02064-x
- 951 62. Hellwig B, Häußler S, Schelter B, Lauk M, Guschlbauer B, Timmer J, Lücking CH. Tremor-
952 correlated cortical activity in essential tremor. *The Lancet*. 2001 Feb 17;357(9255):519-23. DOI:
953 10.1016/s0140-6736(00)04044-7

- 954 63. Roy A, Coombes SA, Chung JW, Archer DB, Okun MS, Hess CW, Wagle Shukla A,
955 Vaillancourt DE. Cortical dynamics within and between parietal and motor cortex in essential
956 tremor. *Movement Disorders*. 2019 Jan;34(1):95-104. DOI: 10.1002/mds.27522
- 957 64. Schuurman PR, Bosch DA, Bossuyt PM, Bonsel GJ, Van Someren EJ, De Bie RM, Merkus
958 MP, Speelman JD. A comparison of continuous thalamic stimulation and thalamotomy for
959 suppression of severe tremor. *New England Journal of Medicine*. 2000 Feb 17;342(7):461-8.
960 DOI: 10.1056/NEJM200002173420703
- 961 65. Louis ED. Linking essential tremor to the cerebellum: neuropathological evidence. *The*
962 *Cerebellum*. 2016 Jun;15:235-42.
- 963 66. Cagnan H, Pedrosa D, Little S, Pogosyan A, Cheeran B, Aziz T, Green A, Fitzgerald J, Foltynic
964 T, Limousin P, Zrinzo L. Stimulating at the right time: phase-specific deep brain stimulation.
965 *Brain*. 2017 Jan 1;140(1):132-45. DOI: 10.1093/brain/aww286
- 966 67. Reis C, He S, Pogosyan A, Haliasos N, Low HL, Misbahuddin A, Aziz T, Fitzgerald J, Green
967 AL, Denison T, Cagnan H. Phase-specific Deep Brain Stimulation revisited: effects of
968 stimulation on postural and kinetic tremor. *medRxiv*. 2022 Jun 21:2022-06. DOI:
969 10.1101/2022.06.16.22276451
- 970 68. Buijink AW, van der Stouwe AM, Broersma M, Sharifi S, Groot PF, Speelman JD, Maurits
971 NM, van Rootselaar AF. Motor network disruption in essential tremor: a functional and
972 effective connectivity study. *Brain*. 2015 Oct 1;138(10):2934-47.
- 973 69. Goede LL, Oxenford S, Kroneberg D, Meyer GM, Rajamani N, Neudorfer C, Krause P, Lofredi
974 R, Fox MD, Kühn AA, Horn A. Linking Invasive and Noninvasive Brain Stimulation in
975 Parkinson's Disease: A Randomized Trial. *Movement Disorders*. 2024.
- 976 70. Shirvalkar P, Prosky J, Chin G, Ahmadipour P, Sani OG, Desai M, Schmitgen A, Dawes H,
977 Shanechi MM, Starr PA, Chang EF. First-in-human prediction of chronic pain state using
978 intracranial neural biomarkers. *Nature neuroscience*. 2023 Jun;26(6):1090-9.
- 979 71. Shirvalkar P, Starr PA, Chang EF. Ambulatory Brain Biomarkers of Chronic Pain: Towards
980 Closed Loop Brain Stimulation. *Biological Psychiatry*. 2024 May 15;95(10):S24.
- 981 72. Opri E, Cernera S, Molina R, Eisinger RS, Cagle JN, Almeida L, Denison T, Okun MS, Foote
982 KD, Gunduz A. Chronic embedded cortico-thalamic closed-loop deep brain stimulation for the
983 treatment of essential tremor. *Science translational medicine*. 2020 Dec 2;12(572):eaay7680.
984